Molecular Therapy
Original Article

Safety concern of recombination between self-amplifying mRNA vaccines and viruses is mitigated *in vivo*

Tessy A.H. Hick,[1,5] Corinne Geertsema,[1,6] Wilson Nguyen,[2,6] Cameron R. Bishop,[2,6] Linda van Oosten,[1] Sandra R. Abbo,[1] Troy Dumenil,[2] Frank J.M. van Kuppeveld,[3] Martijn A. Langereis,[3] Daniel J. Rawle,[2] Bing Tang,[2] Kexin Yan,[2] Monique M. van Oers,[1] Andreas Suhrbier,[2,4] and Gorben P. Pijlman[1]

[1]Laboratory of Virology, Wageningen University and Research, Wageningen, the Netherlands; [2]Inflammation Biology Group, QIMR Berghofer Medical Research Institute, Brisbane, QLD 4029, Australia; [3]Department of Infectious Diseases and Immunology, Utrecht University, Utrecht, the Netherlands; [4]Global Virus Network Centre of Excellence, Australian Infectious Diseases Research Centre, Brisbane, QLD 4072 and 4029, Australia

Self-amplifying mRNA (SAM) vaccines can be rapidly deployed in the event of disease outbreaks. A legitimate safety concern is the potential for recombination between alphavirus-based SAM vaccines and circulating viruses. This theoretical risk needs to be assessed in the regulatory process for SAM vaccine approval. Herein, we undertake extensive *in vitro* and *in vivo* assessments to explore recombination between SAM vaccine and a wide selection of alphaviruses and a coronavirus. SAM vaccines were found to effectively limit alphavirus co-infection through superinfection exclusion, although some co-replication was still possible. Using sensitive cell-based assays, replication-competent alphavirus chimeras were generated *in vitro* as a result of rare, but reproducible, RNA recombination events. The chimeras displayed no increased fitness in cell culture. Viable alphavirus chimeras were not detected *in vivo* in C57BL/6J, *Rag1*$^{-/-}$ and *Ifnar*$^{-/-}$ mice, in which high levels of SAM vaccine and alphavirus co-replicated in the same tissue. Furthermore, recombination between a SAM-spike vaccine and a swine coronavirus was not observed. In conclusion we state that although the ability of SAM vaccines to recombine with alphaviruses might be viewed as an environmental safety concern, several key factors substantially mitigate against *in vivo* emergence of chimeric viruses from SAM vaccine recipients.

INTRODUCTION

mRNA vaccines have emerged as a novel technology during the SARS-CoV-2 pandemic, with 100s of millions globally receiving one or more COVID-19 mRNA vaccinations (e.g., Pfizer-BioNTech, BNT162b2; Moderna, mRNA-1273). A further development for this technology is self-amplifying mRNA (SAM) vaccines,[1–5] a number of which are in clinical trials (Table 1) and three having progressed to licensure. A SAM vaccine against porcine epidemic diarrhea virus (PEDV) (iPED+, Harrisvaccines) was the first to receive licensing in the US, with over 2 million doses prescribed by veterinarians for use in swine.[6–8] This technology was acquired by Merck/MSD Animal Health and forms the basis of the Sequivity vaccine platform (Prescription Product, RNA Particle), which is based on SAM vaccine packaged in a so-called virus-like replicon particle (VRP).[9] GEMCOVAC-19 (Gennova Biopharmaceuticals), a human COVID-19 SAM vaccine,[10,11] was granted "Primary vaccination series for Restricted Use in Emergency Situation" by Indian regulators in 2022.[12] The human COVID-19 SAM vaccine ARCT-154 (Arcturus Therapeutics) received full approval by Japanese authorities in 2023.[13] In contrast to the early SAM vaccines packaged in VRPs, these COVID-19 SAM vaccines are formulated in lipid nanoparticles (LNPs) (Table 1).

SAM vaccines exploit the ability of alphavirus non-structural proteins (nsPs) to amplify mRNA in cells of the vaccine recipient. Vaccine antigen mRNA and protein levels are thereby amplified providing a dose sparing vaccine option.[1,4,14] The nsPs can be derived from several alphaviruses, although most advanced SAM vaccines use the nsPs of the live-attenuated investigational Venezuelan equine encephalitis virus (VEEV) vaccine strain TC-83 (Table 1), which has been administered to thousands of humans, primarily laboratory workers and military personnel.[15,16] TC-83 is also available in Mexico and some South American countries as a registered veterinary vaccine for horses (Equivac TC-83).[17]

The alphavirus nsPs are translated from the positive strand RNA (+RNA/mRNA) as a polyprotein and cleaved into nsP1, nsP2, nsP3, and nsP4 (the RNA-dependent RNA polymerase), which

Received 14 November 2023; accepted 14 June 2024;
https://doi.org/10.1016/j.ymthe.2024.06.019.

[5]Present address: Department of Clinical Microbiology, Umeå University, Umeå, Sweden

[6]These authors contributed equally

Correspondence: Andreas Suhrbier, Inflammation Biology Group, QIMR Berghofer Medical Research Institute, Brisbane, QLD 4029, Australia.
E-mail: andreas.suhrbier@qimrberghofer.edu.au
Correspondence: Gorben P. Pijlman, Laboratory of Virology, Wageningen University and Research, Wageningen, the Netherlands.
E-mail: gorben.pijlman@wur.nl

Table 1. Clinical trials of alphavirus-based SAM vaccines

Alphavirus-based vector	Target	Delivery platform	Enrollment	Institute/Company	Clinical trial phase and number
?	influenza virus	?	468*	Pfizer	phase 1 NCT05227001 (2022–2023*)
SFV4	HPV (TCV)	VRP	12	UMCG, Dutch Cancer Society, and ViciniVax	phase 1 NCT03141463 (2017-2017)[92]
Attenuated VEEV	CEA (6D) (TCV)	VRP	28	AlphaVax	phase 1 and 2 NCT00529984 (2007–2010)[93]
Attenuated VEEV	HCMV	VRP	40	AlphaVax	phase 1 and 2 NCT00439803 (2007–2008)[94]
Attenuated VEEV	HIV	VRP	48 and 96	AlphaVax	phase 1 NCT00063778 (2003–2005) NCT00097838 (2004–2009)[95]
Attenuated VEEV	influenza virus	VRP	216 and 28	AlphaVax	phase 1 and 2 NCT00440362 (2007–2007) NCT00706732 (2008–2009)
VEE vector	neo-antigen (TCV)	LNP	214*	Gritstone bio	phase 1 and 2 NCT03639714 (2019–2023*)[96]
VEEV TRD	SARS-CoV-2	LNP	192	Imperial College London	phase 1 ISRCTN17072692 (2020–2021)[97,98]
VEEV TC-83	SARS-CoV-2	LNP	581	Arcturus Therapeutics	phase 2 NCT04668339 (2021–2022)
VEEV TRD	SARS-CoV-2	LNP	42*	MRC/UVRI and LSHTM Uganda Research Unit	phase 1 NCT04934111 (2021–2022*)
VEE vector	SARS-CoV-2	LNP	81	NIAID and Gritstone bio	phase 1 NCT04776317 (2021–2023*)[1]
VEEV TC-83	SARS-CoV-2	LNP	72*	Arcturus Therapeutics	phase 1 and 2 NCT05037097 (2021–2023*)
VEEV TC-83	SARS-CoV-2	LNP	19400*	Vinbiocare and Arcturus Therapeutics	phase 1, 2, and 3 NCT05012943 (2021–2023*)
VEEV TC-83	SARS-CoV-2	LNP	90*	SENAI CIMATEC	phase 1 NCT04844268 (2022-2022*)
VEE vector	SARS-CoV-2	LNP	340*	Gritstone bio	phase 1 NCT05435027 (2022–2023*)
VEEV TC-83	SARS-CoV-2	LNP	63*	HDT Bio	phase 1 NCT05132907 (2022–2023*)
VEEV TC-83	SARS-CoV-2	LNP	300*	Azidus Brasil and SENAI CIMATEC	phase 2 NCT05542693 (2023-2023*)
VEE vector	SARS-CoV-2	LNP	120*	Gritstone bio	phase 1 NCT05148962 (2021–2024*)
VEEV TRD/SINV	Rabies virus	CNE	82	GSK	phase 1 NCT04062669 (2021–2022)
VEEV TRD/SINV	SARS-CoV-2	LNP	10	GSK	phase 1 NCT04758962 (2021–2022)[99]

?, the nature of the alphavirus-based SAM and delivery platform not provided; *, estimated; CNE, cationic nano emulsion; GSK, GlaxoSmithKline Biologicals; HCMV, human cytomegalovirus; HIV, human immunodeficiency virus; HPV, human papillomavirus; LNP, lipid nanoparticle; NIAID, National Institute of Allergy and Infectious Diseases; SFV, Semliki Forest virus; SARS-CoV-2, severe acute respiratory syndrome coronavirus 2; SINV, Sindbis virus; TCV, therapeutic cancer vaccine; UMCG, University Medical Center Groningen; VEEV, TC-83; TC-83-SINV, recombinant replicon vector contains the TC-83 5′ UTR and non-structural genes and SINV 3′ UTR[72]; VRP, virus-like replicon particle.

self-assemble into an RNA replication complex.[18,19] This "replicase" generates a negative strand RNA intermediate, which is used as a template for +RNA synthesis.[20,21] Importantly, this also initiates synthesis of subgenomic +RNA from the subgenomic 26S promoter located at the 3′ end of the nsP4 gene region on the –RNA.[22] In wild-type (WT) alphaviruses, the subgenomic +RNA encodes the alphavirus structural proteins, whereas in a SAM vaccine this sequence is replaced by a gene of interest (GOI),[5] usually a vaccine antigen or (as used herein) fluorescent reporter genes such as mCherry or nLuc. No alphaviral structural genes are encoded in the SAM vaccine RNA, therefore no infectious viruses are generated and no spreading viral infection can be initiated after SAM vaccination.[23]

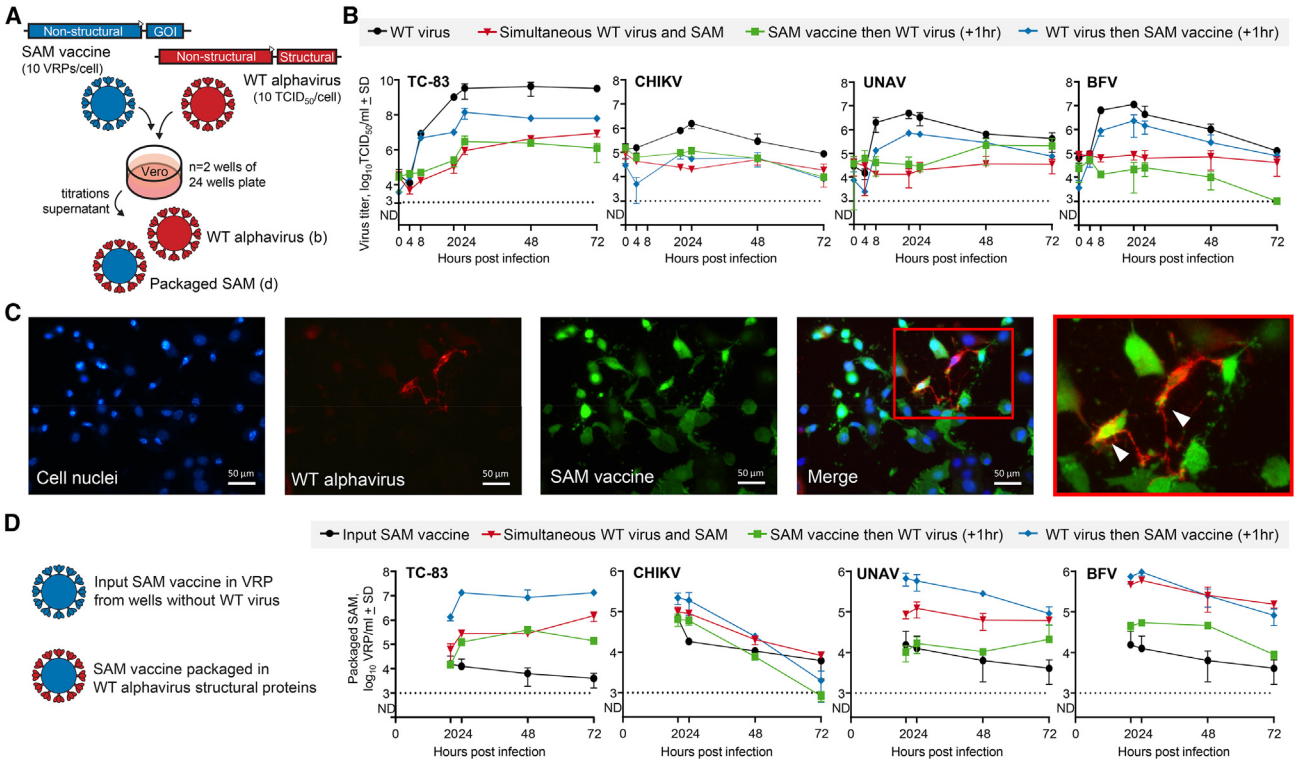

Figure 1. SAM vaccine-induced alphavirus superinfection exclusion

(A) Schematic of experimental set-up; Vero cells were transduced with SAM (10 VRPs/cell) and infected with WT alphaviruses (10 $TCID_{50}$/cell), either at the same time or with a 1 h delay between SAM and WT alphavirus. Supernatant fractions were collected and titrated to quantify (B) the WT alphavirus progeny and (D) the level of SAM vaccine packaged in WT alphavirus particles. (B) WT alphavirus growth kinetics quantified as packaged WT alphavirus genomes (n = 2, detection limit 3 $\log_{10}TCID_{50}$/mL). (C) Fluorescence microscopy of co-transduced/infected Vero cell; cell nuclei stained with Hoechst, WT alphavirus (CHIKV) stained with rabbit anti-CHIKV E2 antibody, and SAM vaccine mCherry expression (recolored green). Co-expression of SAM and WT alphavirus in the same cell is indicated in the enlargement using arrowheads. (D) Titer of SAM packaged in WT alphavirus particles based on SAM-encoded mCherry expression in serial dilutions of supernatant samples (n = 2, detection limit 3 $\log_{10}$VRP/mL).

Alphavirus RNA has been shown in various settings to be able to recombine. For instance, western equine encephalitis virus likely arose from an ancient recombination event between an eastern equine encephalitis-like virus and a Sindbis-like virus.[24] More recently, Mayaro virus (MAYV) recombinants from Brazil and Haiti were reported,[25] with recombination between chikungunya virus (CHIKV) clades also proposed.[26] Numerous *in vitro* and *in vivo* studies have also illustrated the propensity for alphaviruses templates to recombine, specifically during the production of VRPs.[27–33] These VRPs encapsulate SAM in single-cycle delivery vehicles. The first-generation of VRPs were manufactured in mammalian cells by expressing the alphavirus structural proteins from a single co-transfected helper RNA (encoding the structural proteins capsid, E3, E2, 6K and E1), with only the co-expressed SAM packaged into the VRPs. This repeatedly resulted in recombination between SAM and helper RNA, generating replication competent alphaviruses.[34] To avoid this, "split-helper" systems were developed whereby the structural genes were expressed from two separate helper RNAs, which increased the number of required independent recombination events to reconstitute a full-length, infectious alphavirus.[23]

The ability of alphaviruses to recombine presents a theoretical risk for SAM vaccines.[5,35] WT circulating alphaviruses might infect a recent SAM vaccine recipient, thereby providing the opportunity for the generation of a novel chimeric alphavirus comprising the structural genes of the WT alphavirus, and some or all of the non-structural genes of the SAM vaccine. Since alphaviruses can cause serious disease symptoms, ranging from encephalitis to arthritis, such chimera could present a serious health concern and/or environmental risk.[36] Herein, we undertake extensive *in vitro* and *in vivo* assessments to explore recombination between a TC-83-based SAM vaccine and a selection of WT alphaviruses. We also investigate the possibility of a WT coronavirus acquiring a novel coronavirus vaccine antigen from a co-replicating SAM vaccine.

RESULTS

Superinfection exclusion mitigates against co-replication

Recombination between a SAM vaccine and WT alphavirus RNA would ostensibly need both RNA entities to be replicating in the same cell. A phenomenon known as superinfection exclusion, whereby prior infection by one virus blocks subsequent infection by a similar virus, is well described for alphaviruses.[37,38] To determine

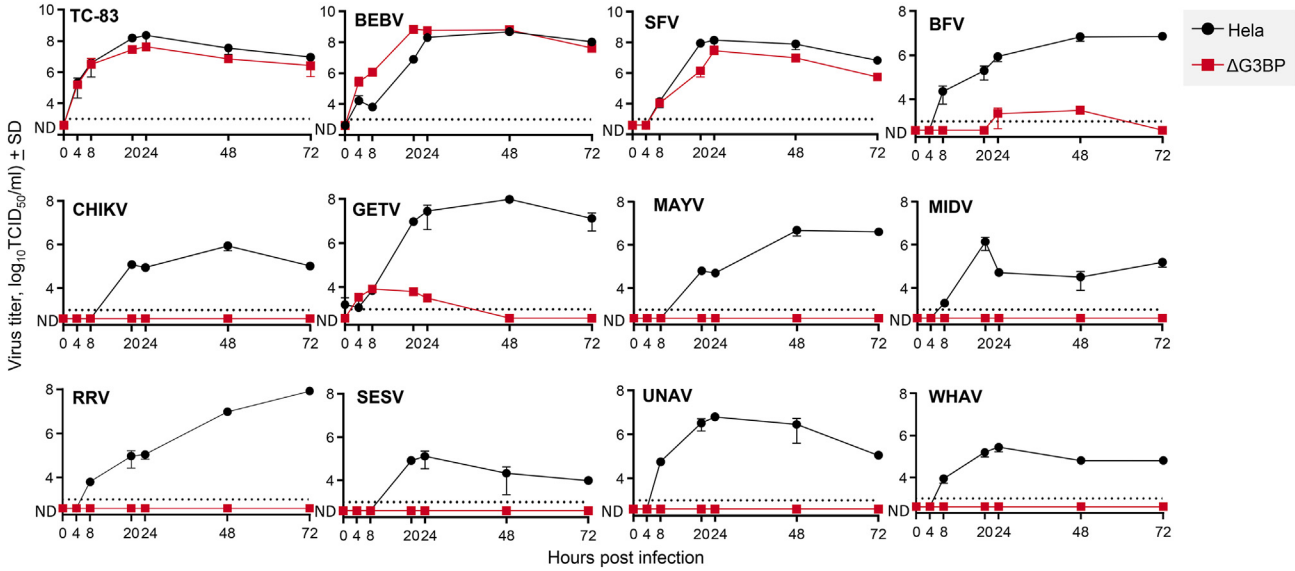

Figure 2. Alphavirus replication kinetics on HeLa ΔG3BP cells

(A) HeLa and HeLa ΔG3BP cells were infected with various alphaviruses (0.1 $TCID_{50}$/cell, $n = 2$). Supernatant fractions were collected and titrated to determine alphavirus growth kinetics (detection limit 3 $log_{10}TCID_{50}$/mL).Venezuelan equine encephalitis virus TC-83 (TC-83), bebaru virus (BEBV), and Semliki Forest virus (SFV) demonstrated to replicate independently of G3BP, whereas Barmah Forest virus (BFV), chikungunya virus (CHIKV), getah virus (GETV), Mayaro virus (MAYV), Middelburg virus (MIDV), Ross River virus (RRV), southern elephant seal virus (SESV), Una virus (UNAV), and Whataroa virus (WHAV) required the presence of G3BP for efficient virus replication.

if SAM vaccines can also mediate superinfection exclusion, Vero cells were transduced with VRPs encapsulating SAM encoding mCherry (SAM-mCherry) at a multiplicity of infection (MOI) of 10 VRPs/cell and infected at a MOI of 10 $TCID_{50}$/cell with WT alphaviruses; specifically, Barmah Forest virus (BFV), CHIKV, and Una virus (UNAV) (Figure 1A). When SAM transduction and alphavirus infection occurred simultaneously, WT alphavirus titers were reduced by up to ≈3 log_{10} (Figure 1B, red). The suppression was similar if SAM transduction was performed 1 h before WT alphavirus infection (Figure 1B, green), but was less effective if the alphavirus was added before the SAM vaccine (Figure 1B, blue). Such reduced superinfection was largely retained when alphaviruses were added at a lower MOI of 1 $TCID_{50}$/cell (Figure S1A). In all cases, the SAM-encoded mCherry reporter was robustly expressed in the majority of cells due to the powerful expression kinetics of the TC-83 nsPs.[39] Thus, the SAM vaccine is able to reduce superinfection, consistent with a role for nsPs in this phenomenon,[37,38,40] but does not completely exclude the superinfecting virus.

Despite the ability to mediate superinfection exclusion, co-expression of SAM and WT alphavirus proteins was observed in a small number of cells (~7%) by fluorescence microscopy (Figures 1C and S1B). Furthermore, in the supernatants of such co-infected/transduced Vero cells (Figure 1A), SAM packaged (or mobilized) with the structural proteins of the WT alphaviruses could also be readily detected (Figure 1D). In the same way in which SAM vaccine VRPs are generated using helper mRNAs, here structural proteins were provided by infection with the WT alphaviruses. As might be expected, given TC-83 RNA is packaged by TC-83 structural proteins, TC-83 infection provided the most efficient SAM packaging, with up to ≈7 log_{10}/mL of packaged SAM particles detected (Figure 1D). CHIKV, UNAV, and BFV infections also resulted in packaging of SAM via a process of cross-packaging[41,42]; albeit slightly less efficiently (Figure 1D). These experiments also illustrated that SAM transduction 1 h after WT alphavirus infection provided the highest level of co-replication, as shown by the high level of SAM packaging (Figure 1D).

Thus, superinfection exclusion can substantially mitigate against RNA co-replication of SAM vaccine and WT alphavirus in the same cell. However, in Vero cells *in vitro* using high MOIs and appropriate timing, superinfection exclusion can, to a certain extent, be overcome.

Generation of replication competent, chimeric alphaviruses by *in vitro* RNA recombination between SAM vaccine and getah virus

To provide optimal conditions for co-infection/transduction and thus potential recombination events, the 1 h delay between SAM-mCherry VRP transduction and WT alphavirus infection was used (as in Figure 1D, blue). The generation of chimeric alphaviruses was evaluated by transferring supernatants from co-infected/transduced Vero cells to HeLa and HeLa GTPase-activating protein (SH3 domain)-binding protein knockout (ΔG3BP) cells (Figure S2). Although WT alphaviruses replicate in HeLa cells, replication of multiple alphaviruses is not supported in HeLa ΔG3BP cells (Figure 2) due to G3BP host factor dependence.[43–45] Of a large panel of 12 alphaviruses, only TC-83, Bebaru virus and Semliki Forest virus were able to replicate in HeLa

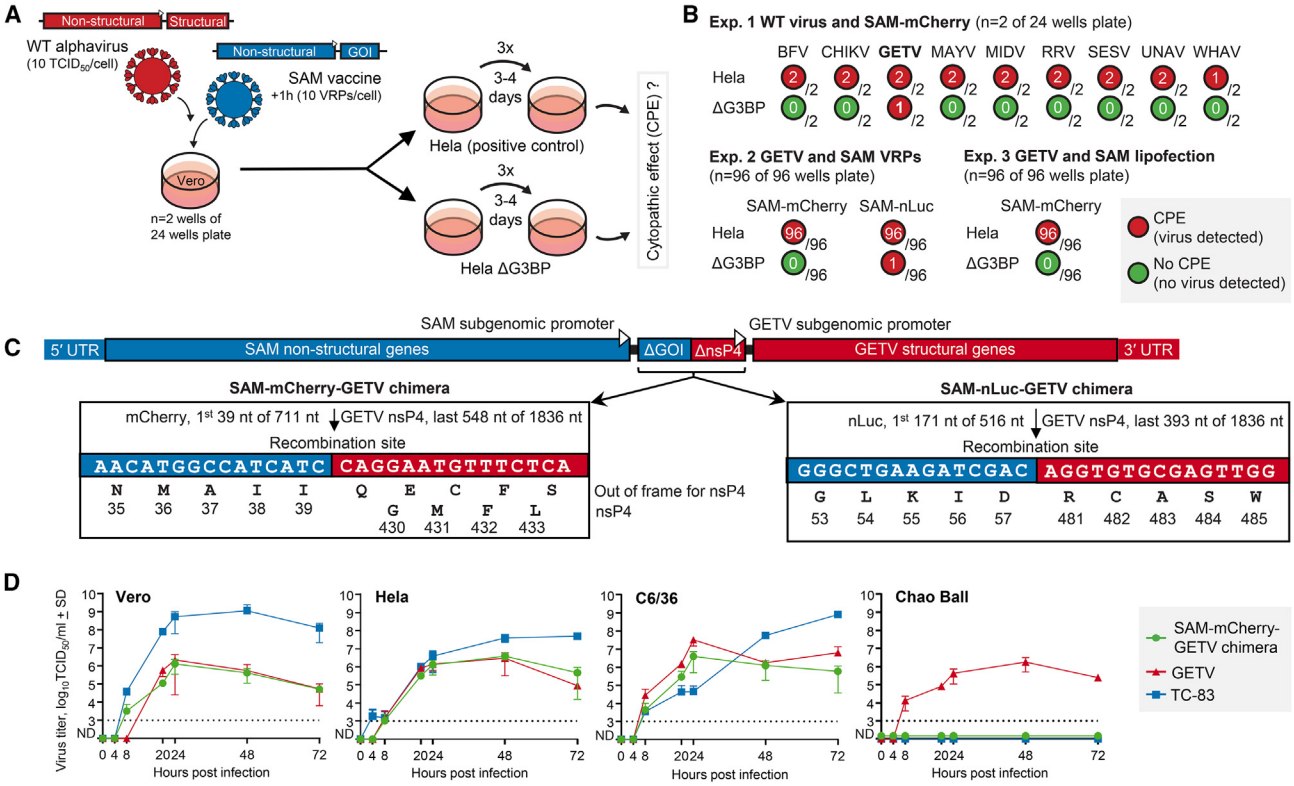

Figure 3. *In vitro* recombination between SAM vaccine and WT alphavirus

(A) Schematic of experimental set-up. Vero cells were infected with WT alphaviruses and transduced with SAM vaccine. After 72 h, supernatants were serial passaged a total of four times (every 3–4 days) on HeLa and HeLa ΔG3BP cells, with CPE monitored by inverted bright-field microscope. (B) WT alphaviruses induced CPE in HeLa cells, but cannot replicate and induce CPE in HeLa ΔG3BP cells. CPE in HeLa ΔG3BP cells (ΔG3BP) indicated the likely presence of a chimeric alphavirus. In the first experiment in 24-well plates, 1/2 wells showed CPE for the combination GETV and SAM encoding mCherry (SAM-mCherry). In the second experiment in 96-well plates, 1/96 wells showed CPE for GETV and SAM-nLuc. (C) Schematic of the two chimeric alphavirus sequences (not to scale), with flanking sequences of the recombination sites. The predicted amino acid sequences are provided, although whether the SAM subgenomic promoter is active is unknown. (D) The replication kinetics of the SAM-mCherry-GETV chimera compared with TC-83 and GETV in Vero (*Cercopithecus aethiops*), HeLa (*Homo sapiens*), C6/36 (*Aedes albopictus*), and Chao Ball (*Culex tarsalis*) cells infected with 0.1 $TCID_{50}$/cell (n = 2). Virus titers determined by serial dilution assays (detection limit 3 $\log_{10}TCID_{50}$/mL).

ΔG3BP cells (Figure 2), with TC-83 data consistent with previous studies demonstrating that its nsP3-hypervariable domain provides G3BP independence.[46] The same phenotypes were observed in U2OS-ΔG3BP cells (Figure S3). The supernatants from the co-infected/transduced Vero cells were then serially passaged for three times in HeLa or HeLa ΔG3BP cells, while virus replication was noted by cytopathic effects (CPE) (Figure 3A). Thus, a viable chimeric alphavirus derived from the TC-83-based SAM should contain, at minimum, the TC-83 nsP3-hypervariable domain and the structural proteins from a G3BP-dependent WT alphavirus. Such chimera will be detected by CPE in ΔG3BP cells. The sensitivity of this assay is illustrated in Figure S4B.

Initially, a set of BFV, CHIKV, and UNAV infections at different MOIs (Figure S4C), orders of infection (Figure S4C), and in different cells (Figure S4D) were screened for recombination with SAM. All combinations failed to generate a chimeric alphavirus capable of inducing CPE in ΔG3BP cells. Subsequently, a set of nine G3BP-dependent alphavirus infections, i.e., BFV, CHIKV, UNAV, Getah virus (GETV), MAYV, Middelburg virus (MIDV), Ross River virus (RRV), Southern elephant seal virus (SESV), Whataroa virus (WHAV), followed by addition of SAM, at 1 h post infection, were screened for recombination in HeLa ΔG3BP (Figure 3B) and U2OS ΔG3BP (Figure S4E) cells. CPE was observed in 1 out of 2 wells (24-well plate) containing HeLa ΔG3BP cells that had received supernatant from Vero cells infected with GETV and were transduced with a SAM encoding mCherry as the GOI (Figure 3B, Exp. 1).

The experiment was then repeated using only GETV, in 96-well plates, in combination with SAM-mCherry and with an additional SAM vaccine that encoded nano luciferase (SAM-nLuc) as the GOI. For Exp. 2, 1 well out of 96 wells showed CPE for the SAM-nLuc/GETV combination (Figure 3B, Exp. 2), whereas none of the 96 wells with SAM-mCherry/GETV combinations showed CPE in the HeLa ΔG3BP cells. Accordingly, recombination is rare and does not depend on the GOI, present in the SAM.

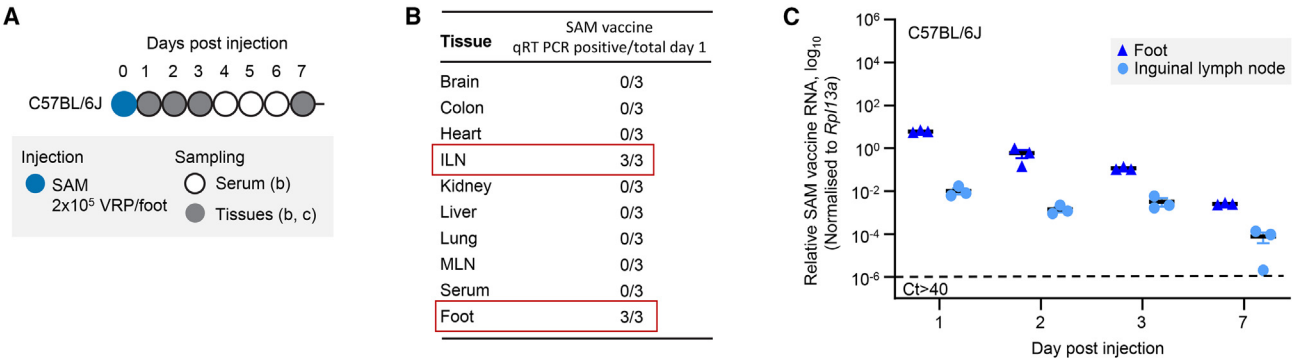

Figure 4. Tropism and persistence of SAM vaccine *in vivo*

(A) C57BL/6J mice were injected subcutaneously into the hindfeet with SAM vaccine (SAM-mCherry, 2×10^5 VRPs/foot). (B) One day post injection, only inguinal lymph nodes (ILNs) and feet were positive for SAM vaccine by nsP2 sequence qRT-PCR detection. (C) qRT-PCR illustrated that the majority of SAM was retained in the feet with ≈1/100 disseminating to the draining inguinal lymph nodes. The cut-off for detection by PCR was Ct > 40.

Finally, the experiment was repeated with lipid-mediated delivery of the SAM vaccine, as current RNA vaccines are usually delivered by LNPs rather than VRPs. SAM-mCherry was formulated in LNP lipid mix but showed insufficient transduction efficiency *in vitro*, therefore Lipofectamine 2000 lipofection was used (Figure S4F). The combination between GETV infection and SAM-mCherry lipofection did not result in CPE in HeLa ΔG3BP cells (Figure 3B, Exp. 3).

The generation of SAM-GETV chimeras (Figure 3B) was confirmed by RT-PCR and western blotting (Figures S4G and S4H). RNA sequencing (RNA-seq) of clarified culture supernatants revealed that both chimeras contained recombination sites within the GOI (mCherry or nLuc) of the SAM construct and nsP4 from GETV, with both subgenomic promoters of SAM and GETV retained, and heterologous 5′ and 3′ UTRs (Figure 3C).

Replication fitness of the chimeric alphavirus

To assess replication fitness, growth of SAM-mCherry/GETV chimera was compared with TC-83 and GETV in mammalian (Vero, HeLa) and mosquito (C6/36, Chao Ball) cell lines. In all cell lines, by 48–72 h post infection, the titer of the chimera was >1 log lower than the attenuated TC-83 vaccine (Figure 3D). Novel features of the chimera (such as heterologous 5′ and 3′ UTRs and/or the two subgenomic promoters) may contribute to this reduced replicative ability. The chimera also never grew to significantly higher titers than GETV (Figure 3D), illustrating that the TC-83 replication machinery provided no growth advantage over GETV in cell cultures. No replication of TC-83 or the chimera was detected in the Chao Ball cells (*Culex tarsalis*) (Figure 3D), even though *Culex tarsalis* is a known vector for VEEV.

Co-replication of SAM vaccine and GETV in mouse tissues

Before the *in vivo* SAM vaccine and alphavirus co-replication experiments, the tropism and persistence of a SAM-mCherry (delivered as VRPs) was determined upon bilateral, subcutaneous injection in the hindfeet of adult C57BL/6J mice (Figure 4A). One day post injection, SAM was detected in the inguinal lymph nodes and at the site of injection, but not in other tissues or serum (Figure 4B). The dispersal to the inguinal lymph nodes may, in part, be due to the tropism of the VRPs for residential dendritic cells at the site of injection, with these cells then migrating to draining lymph nodes.[47–49] The SAM was approximately 2 logs more abundant at the site of injection than in the local lymph nodes, and remained detectable for at least 7 days (Figure 4C).

To examine whether RNA recombination between a SAM vaccine and a WT alphavirus might occur *in vivo*, SAM-mCherry VRPs were mixed with GETV and co-injected subcutaneously into the hindfeet of adult WT C57BL/6J mice, recombination-activating gene 1-deficient (*Rag1*$^{-/-}$) mice, and type I interferon (IFN) receptor-deficient (*Ifnar*$^{-/-}$) mice (Figure 5A). Hindfeet were chosen as they are a few degrees cooler than core body temperatures (36°C–37°C), which results in depressed type I IFN responses and thus increased alphavirus replication in foot tissues of C57BL/6J[50] and likely also *Rag1*$^{-/-}$ mice. C57BL/6J mice represent a standard model for alphavirus arthritis[51,52] with brief viremia. *Rag1*$^{-/-}$ mice, which lack functional B and T cells, provide a model of persistent viremia[52,53] and *Ifnar*$^{-/-}$ mice provide a lethal model, with high level viremia[54,55] (Figure 5B). The inclusion of GETV did not have a major impact on the presence of SAM; both SAM and GETV RNAs were simultaneously detected in feet and inguinal lymph nodes with substantially higher levels in *Ifnar*$^{-/-}$ mice (Figure S5).

No evidence for the generation of chimeric alphaviruses *in vivo*

Mice were bled and/or euthanized and tissues harvested at the indicated days post infection/transduction (Figure 5A). Serum viremias developed as expected (Figure 5B). The putative generation of chimeric alphaviruses in mice was investigated by sequencing the polyadenylated RNA in feet using a stranded, 75 bp paired-end read approach. Sequencing reads were aligned to references including the mouse (GRCm38 vM26), GETV, and SAM sequences. Of the ≈384 million aligned read pairs (across all samples),

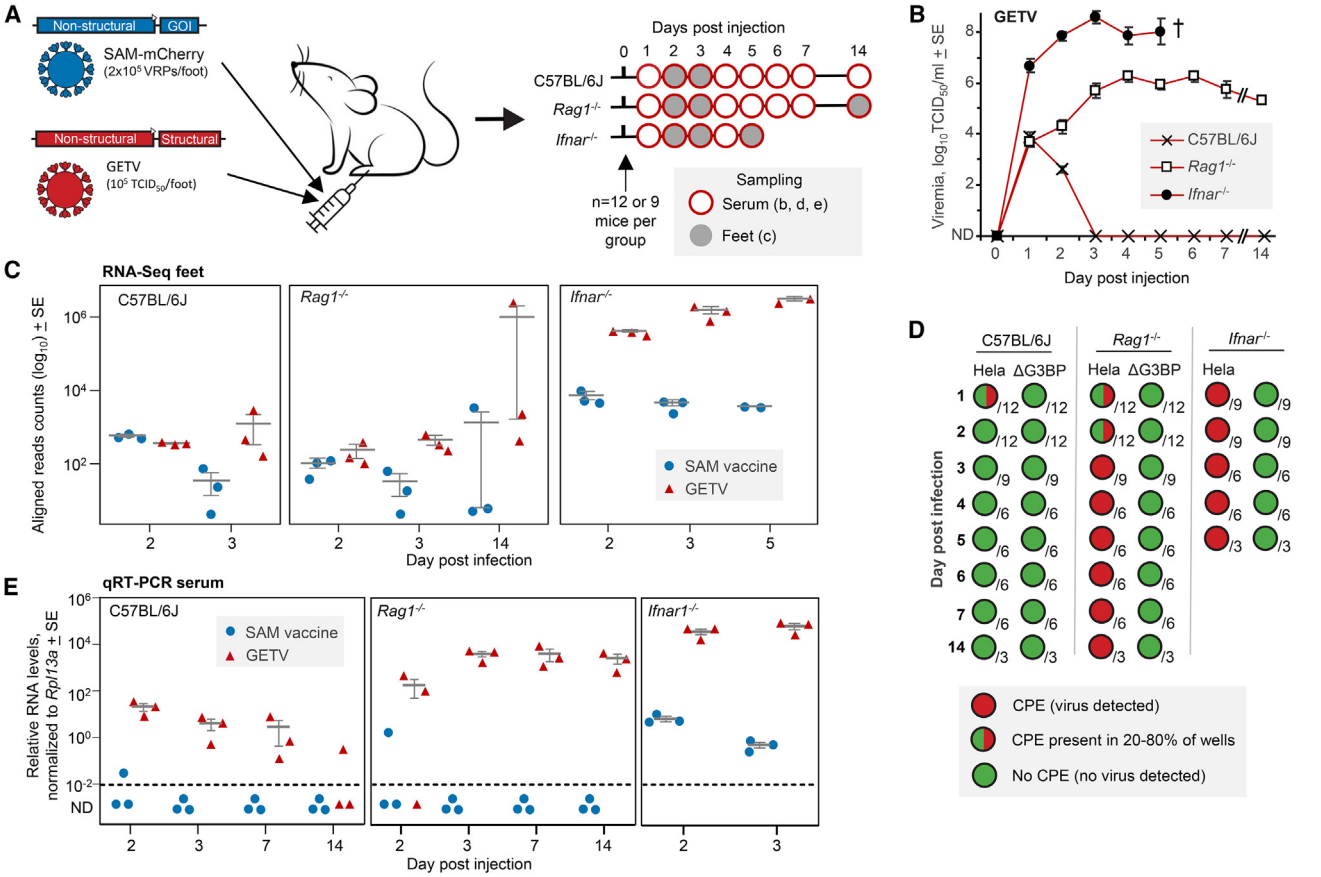

Figure 5. *In vivo* SAM vaccine and GETV co-injection

(A) Schematic of experimental set-up. SAM vaccine encoding mCherry and GETV were co-injected subcutaneously into hindfeet of C57BL/6J, *Rag1*$^{-/-}$ and *Ifnar*$^{-/-}$ mice. Serum and feet were collected at the indicated days post injection. (B) GETV viremia in the indicated mouse strains (n = 12 or 9 on day 1 and decrease to n = 3 on day 5 for *Ifnar*$^{-/-}$ mice, and n = 3 on day 14 for C57BL/6J and *Rag1*$^{-/-}$ mice). (C) RNA-seq of feet; counts of reads aligning to the SAM or GETV sequence. (D) Serum samples were passaged a total of four times on HeLa and HeLa ΔG3BP cells. CPE was noted by bright-field inverted microscope with indication of the number of serum samples tested. (E) qRT-PCR of serum samples using primers for SAM and GETV nsP2 sequences.

15,185,006 (≈4%) aligned to the sequence of SAM or GETV (Table S1) and confirmed the simultaneous presence of SAM and GETV in foot tissues (Figure 5C). As expected, the number of reads aligning to both GETV and SAM vaccine were substantially (>2 logs) higher in *Ifnar*$^{-/-}$ mice (Figure 5C).

We deployed customized bioinformatic processes that identified (from all mice and all time points), only six chimeric read-pairs/reads that contained sequences from both the SAM vaccine and from GETV (Figure S6). Each chimeric read-pair/read was unique and was present as a single copy, illustrating that the chimeric read-pairs/reads were not derived from replicating RNA or replication-competent virus. Negative qPCR on the same samples confirmed that the chimeric reads are indeed artifacts (Figure S7). Most likely the chimeric read-pairs/reads were the result of random template switching during RNA-seq library construction (Figure S6), which produces a low frequency of stochastic, irreproducible artifactual fusion alignments.[56] Similar artifactual chimeric read-pairs were identified for mouse genes on different chromosomes (Figure S8; Table S1). As cross-chromosome mRNA splicing is not a feature of mammalian cells, these chimeric reads were assumed artifacts.[56] As expected for a stochastic process, chimeric reads were more frequent for highly expressed genes (Figures S8B–S8E). As the SAM-GETV chimeric reads had a lower frequency than mouse-mouse chimeric reads (Table S1), and were single copies (Figure S6), they are assumed artifacts created during RNA-seq library preparation.[56]

In addition to RNA-seq, serum samples collected at the indicated times (Figure 5A) were examined for the presence of chimeras by passaging the samples on HeLa and HeLa ΔG3BP cells as described previously (Figure 3A). As expected, GETV present in serum samples caused CPE in HeLa cells (Figure 5D). However, no CPE was observed in HeLa ΔG3BP cells for any sample, at any time point, from any mouse strain (Figure 5D). This indicated that a similar chimera as generated *in vitro* (Figure 3C) was not present in the serum samples.

Serum samples were also analyzed by qRT-PCR. GETV RNA was detected for up to 7 days post injection in all C57BL/6J mouse serum samples, consistent with previous data.[57] GETV RNA levels persisted in *Rag1*$^{-/-}$ and were elevated in *Ifnar*$^{-/-}$ mice (Figure 5C), consistent with viremia (Figure 5B). SAM was detected in serum samples of one C57BL/6J and one *Rag1*$^{-/-}$ mouse on day 2, and all *Ifnar*$^{-/-}$ mice on days 2 and 3 (Figure 5E). This indicated the presence of either (1) input SAM vaccine that had escaped the injection site and entered the circulation, (2) SAM packaged/mobilized (as described in Figure 1D) by GETV structural proteins, or (3) a chimeric virus had emerged and generated a low-level viremia. Either of the latter two would indicate co-replication of SAM and GETV in the same cells *in vivo*, illustrating (at a minimum) that this experimental set-up had provided conditions for recombination. However, the actual occurrence of recombination is not supported by the other analyses; a replication-competent chimera was not detected in serum by passaging on HeLa ΔG3BP (Figure 5D) or in feet by RNA-seq (Figure 5C).

No evidence for recombination in the spike gene of a SAM coronavirus vaccine

Distinct from the possibility of recombination between WT alphaviruses and the alphavirus sequences of the SAM vaccine, we investigated the possibility that the SAM vaccine antigen (GOI) could provide recombination opportunities with virus sequences targeted by the vaccine. The advent of COVID-19 SAM vaccines (Table 1) and the well-known ability of coronaviruses to recombine and generate chimeras with increased fitness,[58,59] begged the question of whether a coronavirus could recombine with a SAM vaccine encoding a coronavirus antigen. Recombination between PEDV and a SAM-encoded PEDV spike protein of a different PEDV strain was therefore evaluated. Firstly, *in vitro* conditions (Figure 6A) were established that resulted in the presence of SAM and PEDV in the same cells, specifically PEDV-induced syncytia (Figures 6B, S9A, and S9B).

To assess recombination, we exploited the ability of the PEDV DR13 spike to mediate trypsin-independent infection, due to an R to G substitution at position 890 in the spike S2 domain,[60,61] with PEDV CV777 only able to infect cells *in vitro* in the presence of trypsin (Figure 6C). A series of SAM constructs encoding the PEDV DR13 spike or S2 domain were transfected into Vero cells (Figures 6D and S9C), which were also infected with PEDV CV777 in the presence of trypsin (Figure 6E). Co-replication of SAM and PEDV CV777 did not result in superinfection exclusion, with PEDV CV777 titers largely being unaffected by SAM (Figure 6F). Supernatant samples were transferred onto Vero cells and passaged three additional times in the presence and absence of trypsin (Figure 6G). As expected, CPE occurred in the presence of trypsin due to the replication of PEDV CV777 (Figure 6G, Exp. 1). No CPE was observed in the absence of trypsin (Figure 6G, Exp. 1), despite the sensitivity of the assay (Figure S9D). This indicated that no recombination had occurred between the SAM-DR13 spike/S2 sequence and PEDV CV777 genome to produce a chimeric coronavirus capable of proliferating in the absence of trypsin.

A replication-defective PEDV DR13 RNA template (D-PEDV-DR13)[60,61] (Figure 6D) was included as positive control. Supernatant from cells transfected with this RNA template and infected with PEDV CV777 was able to cause CPE in absence of trypsin (Figure 6G). As expected, recombination between PEDV CV777 and D-PEDV-DR13 resulted in acquisition by PEDV CV777 of trypsin independence from D-PEDV-DR13 (Figure 6G, Exp. 1).

A repeat experiment was undertaken using the expanded 96 wells format, with the expected recombination between PEDV CV777 and D-PEDV-DR13 seen in 4 of 96 wells (Figure 6G, Exp. 2). Again, no PEDV CV777-SAM chimera was generated in any of the 96 wells, capable of replicating in the absence of trypsin (Figure 6G, Exp. 2). Overall, these experiments illustrated that PEDV CV777 was able to acquire genes from a PEDV DR13 RNA template, but not from a SAM-DR13 spike vaccine.

DISCUSSION

Herein, we present the first evidence for rare RNA recombination events between an alphavirus-based SAM vaccine and a WT alphavirus generating replication-competent alphavirus chimeras *in vitro* in Vero cells under optimized conditions. Sequencing indicated a single recombination event in both chimeras between the SAM GOI (mCherry or nLuc) and the GETV nsP4 gene. Both chimeras also retained the subgenomic promoters of the SAM vaccine and GETV. No such recombination events were observed with a series of other alphaviruses under identical conditions. Despite optimizing *in vivo* conditions that would promote recombination and identify recombination events, we were unable to detect replication-competent chimeras in three different mouse models. These included *Ifnar*$^{-/-}$ mice, in which high levels of SAM and GETV were co-expressed in the same tissue. GETV titers in our *in vivo* experiments (up to 10^4 $TCID_{50}$/mL in C57/BL6 mice at 2 dpi, Figure 6B) are comparable with viral titers in natural GETV infection of swine[62] and thus reflect the physiological relevance of our model.

Although the ability of SAM vaccines to recombine with a WT alphavirus might be viewed as a safety concern, a series of factors mitigate against emergence of such entities from SAM vaccinated populations. As shown, superinfection exclusion substantially reduces the probability of SAM and alphavirus replication in the same cell. Furthermore, SAM vaccines induce CPE in mammalian cells,[63] so the number of transduced cells steadily declines post vaccination, although SAM can remain detectable for up to 60 days in primates.[64] Alphavirus viremias are usually cleared within 7 days,[36,65] although again, viral RNA in tissues steadily declines over time, but can remain detectable for up to 100 days.[53,66] Thus, vaccination and infection would need to occur within a limited time frame to provide opportunities for co-replication in the same cell. Arguably the most important consideration is that the high MOIs used *in vitro* to achieve co-infection/transduction and overcome superinfection exclusion, may be difficult to achieve *in vivo*. In addition, infection with an alphavirus ordinarily causes rapid induction of protective neutralizing IgM and IgG antibodies.[53,65] Therefore, if a chimeric alphavirus did emerge in an infected vaccine recipient, it would contain the same

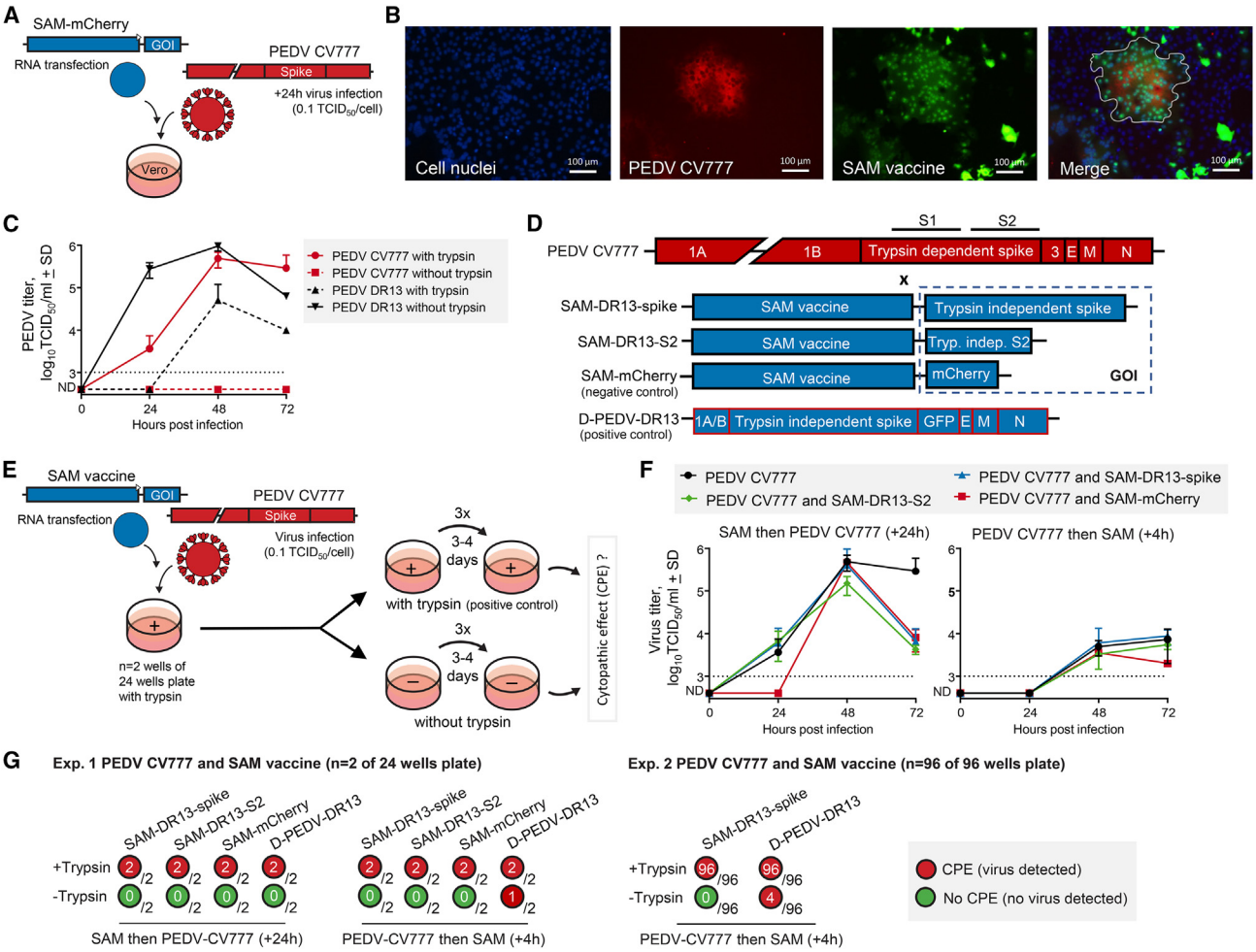

Figure 6. *In vitro* co-introduction of a coronavirus and a SAM vaccine encoding a coronavirus spike

(A) Schematic of experimental set-up (B) Vero cells were transfected with SAM vaccine encoding mCherry and infected with PEDV CV777 (0.1 $TCID_{50}$/cell, 24 h post transfection). (B) Fluorescence microscopy of co-transfected/infected Vero cell; cell nuclei stained with Hoechst, PEDV CV777 stained with mouse anti-PEDV spike, and SAM vaccine mCherry expression (recolored green). Merge showing co-expression of PEDV CV777 and SAM in syncytium (white line). (C) Vero cells were infected with PEDV CV777 or PEDV DR13 (0.1 $TCID_{50}$/cell) in the presence or absence of trypsin ($n = 2$). PEDV titers were determined based on serial dilutions of supernatants samples on Vero cells in the presence of trypsin (detection limit 3 $\log_{10}TCID_{50}$/mL). D, Genome organization of PEDV CV777, three SAM vaccine constructs and a defective PEDV DR13 RNA construct. (E) Schematic of experimental set-up (F and G). The SAM vaccine or defective PEDV DR13 RNA (positive control) constructs were transfected into Vero cells, that were infected with PEDV CV777 (0.1 $TCID_{50}$/cell) 4 h prior or 24 h post transfection. After 72 h incubation in the presence of trypsin, supernatants were serial passaged a total of four times (every 3–4 days) on Vero cells in the presence or absence of trypsin, with CPE monitored by inverted light microscope. (F) Growth kinetics of PEDV CV777, with or without transfection with SAM vaccine constructs ($n = 2$, detection limit 3 $\log_{10}TCID_{50}$/mL). (G) PEDV CV777 induced CPE in Vero cells with trypsin, but cannot replicate and induce CPE in Vero cells without trypsin. CPE in Vero cells without trypsin indicated the likely presence of a chimeric coronavirus. In the first experiment in 24-well plates, 1/2 wells showed CPE for the combination PEDV CV777 and the defective PEDV DR13 RNA (positive control). In the second experiment in 96-well plates, 4/96 wells showed CPE for PEDV CV777 and the defective PEDV DR13 RNA (positive control).

structural proteins as the WT alphavirus and would therefore be subject to neutralization by the same antibodies. Moreover, a chimera needs to achieve a high viremia to be transmitted via mosquito vectors.[67] Transmission via mosquitoes would not be assured, because the SAM-GETV chimera was not able to replicate in a *Culex* cell line, in contrast to GETV (Figure 2D). *Culex* mosquitoes are important vectors for GETV,[68] with a number of barriers within the mosquito to be overcome before transmission can occur.[67,69] Finally, alphavirus outbreaks are usually sporadic, often short-lived and restricted to specific geographical regions,[36,70] again limiting opportunities for infection of SAM vaccine recipients. Nevertheless, regulators may take pause when considering a mass rollout of a SAM vaccine in the middle of a GETV outbreak.

The two SAM-GETV chimeras showed recombination in the GOI of the SAM vaccine and nsP4 gene of GETV, and both retained

the subgenomic promotors of SAM and GETV. Recombination in the vicinity of the subgenomic region has been described previously for defective interfering alphaviruses RNAs.[31] Whether this represents a recombination hot spot remains unclear. As the GOI of the SAM (mCherry or nLuc) and nsP4 of GETV have no sequence similarity, this suggest a mechanism of non-homologous recombination by template switching of the RNA-dependent RNA polymerase, which has been described for alphavirus RNA templates.[27,71] The two promoters may need to be retained to generate a functional virus. As the interaction between the SAM nsP4 and nsP1-3 is highly selective, a non-functional chimera may well be generated when the SAM nsP4 is replaced with the corresponding sequence from GETV.[32] Although the relative activity of the two subgenomic promoters in terms of transcription and translation is unknown, at least one is needed to maintain the optimal ratio of genomic and subgenomic RNA for efficient virus replication.[72] The presence of the two promoters may contribute to the attenuation of the chimera in cell culture.[73]

Our analyses had a few limitations regarding alphavirus combinations. We were unable to assess potential recombination between SAM and the G3BP-independent alphaviruses VEEV, WEEV and EEEV because of biosafety restrictions, and because these viruses do not require G3BP, precluding the use of ΔG3PB cells for detection. The inability to detect other chimeric viruses using the G3BP-dependent alphaviruses BFV, CHIKV, MAYV, MIDV, RRV, SESV, and WHAV (Figure 3B), may argue that viable chimeras cannot readily be generated with these alphaviruses. Key features like regulation of genomic to subgenomic RNA levels, packaging requirements, or compatibility of 5′ and 3′ UTRs might be most optimal for SAM-GETV chimeras.[42,74] However, the probability of chimera formation may simply be low, requiring a larger number of repeat experiments to export further recombination possibilities. Also unclear is whether the immortalized Vero cells (an African green monkey kidney cell line), which is remarkably permissive for replication of many viruses, provides a favorable environment for recombination. Conceivably, such conditions are substantially less favorable in primary cells *in vivo*.

Infection of a SAM vaccine recipient with the very virus targeted by the vaccine, might be viewed as somewhat likely, with, for instance, many recipients of the GEMCOVAC-19 vaccine likely to be infected with SARS-CoV-2. SARS-CoV-2 can recombine to increase fitness, as seen for the XBB variant.[59] However, we were unable to show recombination between a SAM-spike vaccine and a coronavirus, despite establishing an *in vitro* system where recombination between a defective coronavirus RNA and a coronavirus could repeatedly be demonstrated. Conceivably, opportunities for recombination may be limited because SAM and coronavirus RNAs replicate in distinct, virus-induced, subcellular membrane bound structures. Alphaviruses utilize single membrane spherules at the plasma membrane, which are internalized in endosomes and lysosomes to form cytopathic vacuoles.[75,76] In contrast, coronaviruses form double membrane vesicles in the endoplasmic reticulum.[77,78]

There is only one form of recombination that we did not explore; recombination between the SAM-encoded coronavirus spike and alphaviruses, creating a potential coronavirus-alphavirus chimera. Although inter-genus and inter-family recombination events to generate replication competent chimeric viruses have been reported for geminiviruses (plant viruses),[79,80] this is very rare for mammalian RNA viruses[81] and, to the best of our knowledge, has never been reported for an alphavirus. The reasons likely include strict structural protein assembly requirements, RNA packaging constraints, RNA polymerase incompatibilities, and for alphaviruses a propensity to delete heterologous unnecessary sequences.[33]

Current RNA vaccines are usually delivered by LNPs rather than VRPs. VRPs were used herein as they provide high transduction efficiency, thereby avoiding false negative results when very low-frequency events are involved. The lower transduction efficiency of LNPs would likely decrease the probability of detecting recombination events. In addition, as VRPs and GETV use members of low-density lipoprotein receptor family as entry receptors,[82] the probability of co-transduction/infection in the same cell *in vivo* may be lower for LNP delivery. In reality, deployment of a licensed SAM vaccine involves vaccination of millions of individuals, permitting low-frequency events to emerge. That the SAM vaccine delivery modality itself could influence the recombination mechanism seems improbable, with LNP-delivered SAM likely to be as capable of recombination with an alphavirus RNA as VRP-delivered SAM. However, a full exploration of the cell type(s) *in vivo* that show SAM vaccine RNA replication after LNP delivery, and also support alphavirus replication, may be warranted to further explore recombination events.

In summary, we demonstrated recombination events between SAM vaccines and GETV *in vitro*, thereby presenting a potential environmental safety risk for SAM vaccines. However, a series of factors mitigates against generation, emergence, and transmission of chimeric alphaviruses as a result of SAM vaccination.

MATERIALS AND METHODS

Ethics statement and regulatory compliance

Mouse work was conducted in accordance with the Australian code for the care and use of animals for scientific purposes as defined by the National Health and Medical Research Council of Australia. Mouse work was approved by the QIMR Berghofer MRI Animal Ethics Committee (P3746 A2108-612). Details of housing conditions and environmental enrichments have been described previously.[83] The SAM vaccine was imported to QIMR Berghofer MRI from Wageningen University and Research under Australian DAWR Permit no. 0005386925. SAM vaccine work was undertaken in a biosafety level 3 facility at the QIMR Berghofer MRI: Australian Department of Agriculture, Fisheries and Forestry, Approved Arrangement site certification Q2326; and Office of the Gene Technology Regulator certification 3445. Work with the SAM vaccine was approved under Notifiable Low Risk Dealing (NLRD) Identifier; NLRD_Suhrbier_Sept2022: NLRD 2.1(d). Breeding and use of GM mice was approved under NLRD Identifier: NLRD_Suhrbier_Oct2020: NLRD 1.1 (a).

The HeLa and HeLa ΔG3BP cell lines were imported under Australian DAWR Permit no. 0006024827. Work with GETV was conducted under a Queensland Biosecurity Act 2014 permit no PRID 000907.

Cell lines and viruses

HeLa and U2OS G3BP1 and G3BP2 double knockout cells (ΔG3BP) were generated using CRISPR-Cas9.[84] Mammalian cells were cultured in complete medium (DMEM [Gibco], 5%–10% FBS [Gibco], and 1% penicillin-streptomycin [Sigma-Aldrich]) at 37°C in 5% CO_2. Mosquito cells were maintained at 28°C in supplemented medium (Leibovitz L-15 medium, 10% FBS, 2% tryptose phosphate broth, and 1% nonessential amino acids [all Gibco]). Alphavirus stocks of Bebaru virus (MM2354), BFV, CHIKV (S27, MF580946.1), GETV (MM2021, MW404214.1), MAYV (BeH407, MK573238.1), MIDV) (30037), RRV) (T48, GQ433359.1), SESV (HM147990.1), Semliki Forest virus (4, KP699763.1), UNAV (CoAr2380), TC-83 (L01443.1), and WHAV were grown on C6/36 or Vero cells. PEDV CV777 (GenBank JQ023162.1) and PEDV DR13 (GenBank AF353511.1) stocks were grown on confluent Vero cells supplemented with 10 μg/mL trypsin-EDTA (Gibco).

SAM vaccine

The SAM vaccine construct and two split-helper RNA constructs were based on the attenuated VEEV TC-83 strain.[23] In brief, the SAM construct encoded the TC-83 non-structural proteins, the 26S subgenomic promoter, and a multiple cloning site for insertion of the GOI (mCherry, nLuc, PEDV DR13 spike, or PEDV DR13 spike S2 domain sequence). The helper RNA constructs carried the first 195 nucleotides of nsP1 and the capsid or envelope glycoprotein genes.[23] Plasmids encoding the SAM and helper constructs were isolated (NucleoBond Xtra Midi EF purification kit, Macherey-Nagel), linearized (NotI, New England BioLabs), *in-vitro*-transcribed (T7 RNA polymerase, New England BioLabs), and capped (Cap structure analog, New England BioLabs). The capped RNA constructs were co-electroporated (0.4 cm cuvettes, two pulses of 850 V/25 μF using Gene Pulser Xcell [Bio-Rad]) into 8×10^6 BHK-21 cells (clone 13, ECACC 85011433) in 800 μL PBS to produce VRPs, which were harvested from the supernatant 24 h post electroporation. VRPs were quantified by serial dilution of supernatant on Vero cells. After overnight incubation, cells were counted that expressed SAM encoded mCherry or nsP2, by respectively fluorescence microscopy or immunoperoxidase straining with goat anti-TC-83 nsP2 (1:1,000, AlphaVax), rabbit polyclonal anti-goat alkaline phosphatase (1:2,500, Sigma), alkaline phosphatase, and NBT/BCIP (1:50, Roche). Based on the positive cell count and the dilution factor, the VRP titers were determined.

SAM vaccine transduction and WT alphavirus infections *in vitro*

Mammalian cells in 24- or 96-well plates were transduced with SAM vaccine (10 VRPs/cell) and/or infected with WT alphaviruses (1 or 10 $TCID_{50}$/cell). After 1 h, the supernatant was replaced for fresh medium or a sequential SAM vaccine transduction or alphavirus infection. Supernatant samples were collected at indicated time points to determine the alphavirus and packaged SAM titers. Samples were serially diluted on Vero cells. After overnight incubation, cells expressing the SAM-encoded mCherry protein were counted. Based on the fluorescent cell count and the dilution factor, the packed SAM titers were determined. Alphavirus titers were determined by CPE as described.[85] In case of CHIKV infection, 24 h post infection co-expression with the SAM vaccine was examined by immunofluorescence staining using rabbit anti-CHIKV E2 (1:5,000) and goat polyclonal anti-rabbit Alexa Fluor 488 (1:2,000, Invitrogen) as described.[85]

Lipid nanoparticle formulation

In vitro transcribed mRNA of SAM-mCherry was treated with RNase-Free DNase (Promega) and was purified with the RNeasy Midi Kit (QIAGEN). Purified mRNA was formulated in LNPs by hand mixing with ALC-0315 lipid mix in a 5:1 ratio (LNP Trailblazer Kit, Echelon Biosciences) and was diluted 20× in 1× PBS buffer. Vero cells in a 96-well plate were transfected with LNPs (up to 250 ng mRNA per well) in 100 μL volume. After 2 h, the supernatant was replaced for fresh medium. The transfection efficiency was observed by fluorescence microscopy at 24 h post treatment.

WT alphavirus infection followed by SAM-mCherry lipofection

Vero cells in a 96-well plate were first infected with GETV (10 TCID50/cell), followed by SAM-mCherry lipofection at 1 h post infection. Transfection was performed with Lipofectamine 2000 transfection reagent (Invitrogen) with 0.2 μL *in-vitro*-transcribed mRNA per well. After 2 h, the supernatant was replaced for fresh medium. A cell-based alphavirus recombination detection assay was performed by serial passaging the supernatant on HeLa and HeLaΔG3BP cells.

Cell-based alphavirus recombination detection assay

RNA recombination events between SAM vaccine and WT alphaviruses were evaluated by serial passages of supernatant samples collected 72 h post co-introduction, or serum samples collected from mice. Samples were incubated for 3–4 days on HeLa, HeLa ΔG3BP, U2OS, and U2OS ΔG3BP cells, passaged to fresh cell monolayers, and screened for CPE by eye using a light inverted microscope. The sensitivity of the assay was illustrated by using TC-83 and a constructed TC-83-CHIKV chimera (Figures S4A and S4B).

RNA-seq of *in-vitro*-generated SAM-GETV chimeras

SAM-GETV chimeras isolated from HeLa ΔG3BP cells were used to infect Vero cells. 48 h post infection, RNA was purified from supernatant using TRIzol LS reagent (Invitrogen), and direct RNA-seq libraries were generated using the TruSeq Stranded mRNA Library Prep kit (Illumina). Poly(A) containing RNA molecules were purified, fragmented, and copied into cDNA strands. Adapter sequences were ligated at the ends of the cDNA to allow hybridization with sequencing primers. The resulting libraries were sequenced at Utrecht Sequencing Facility (Utrecht University, the Netherlands) on the iSeq 100 platform (2 × 100 bp, Illumina). Resulting Fastq files were trimmed, qualified filtered, *de novo* assembled and aligned to GETV (MM2021 strain, GenBank MN849355) and SAM vaccine reference (Geneious bioinformatics software).

Alphavirus growth kinetics

Alphavirus growth kinetics were determined by alphavirus infection (0.1 $TCID_{50}$/cell) of indicated cell lines. One hour post infection, the infection fluid was removed, cell monolayers were washed with PBS, and fresh medium was added. Viral titers were determined from supernatant samples collected at various time points as described.[85]

SAM vaccine and GETV co-injections *in vivo*

Female 6- to 8-week-old C57BL/6J and *Rag1*$^{-/-}$ (B6.129S7-Rag1tm1-Mom/J) mice were purchased from the Animal Resource Centre, Perth, WA, Australia. *Ifnar*$^{-/-}$ mice on a C57BL/6J background were kindly provided by P. Hertzog (Monash University, Melbourne, Australia)[86] and were bred in-house at the QIMR Berghofer MRI Animal Facility. Female mice (6–10 weeks) were injected subcutaneously into the hindfeet[52] with SAM vaccine (2×10^5 VRPs/foot) mixed with GETV (10^5 $CCID_{50}$/foot).[87] Serum viremia and disease manifestations were monitored as described.[52,87]

Mouse RNA-seq and bioinformatics

RNA from feet was purified and subjected to RNA-seq as described earlier.[51,66,88] The cDNA libraries were sequenced in-house at QIMR Berghofer MRI on the NextSeq 550 platform (2×75 bp, Illumina). Bioinformatics was undertaken as described.[51,89,90] In brief, Fastq files were trimmed to remove sequencing adapters using Trimmomatic version 0.36 and were quality checked using fastQC. Trimmed reads were aligned to a multi-fasta reference sequence consisting of the GETV (MM2021 strain) (GenBank ID: MN849355) genome sequence and the sequence of the SAM vaccine encoding mCherry, using Bowtie2 version 2.2.9 with "–fast-local" settings. Reads were aligned to the GRCm38 version M26 mouse reference sequence using STAR version 2.7.1. The number of primary proper reads aligning to each reference genome was calculated using Samtools version 1.10, and plotted with ggplot2 version 3.3.5 in R version 4.1.0.

qRT-PCR of mouse serum

RNA was extracted from serum samples using TRIzol LS reagent (Invitrogen). qRT-PCR (iTaq Universal SYBR Green Supermix, Bio-Rad) was undertaken using specific TC-83 and GETV primers (TC-83 nsP2 sequence F 5′ACCAAGAAAGCTTGTCTGCATCTG3′, R 5′CTTCAAGTGAGGATTTCGGTTTGC3'; GETV nsP2 F 5′GGAG GGGATTCACTACACCTGC3′, R 5′TTGCTCGTCACACACGCTGG3′), with normalization to housekeeping gene *Rpl13a*.[91]

SAM vaccine transfection and coronavirus infections *in vitro*

The SAM vaccines were transfected (Lipofectamine 2000, Invitrogen) when Vero cell monolayers reached 70% confluence, followed by the PEDV CV777 infection (0.1 $TCID_{50}$/cell) when monolayers reached 100% confluence 24 h post transfection to allow supplementation of trypsin in absence of FBS. In addition, the transfection was performed on 100% confluent Vero cell monolayers 4 h post PEDV CV777 infection (0.1 TCID50/cell) in medium with trypsin. After 2 h incubation, the transfection/infection fluid was replaced with fresh medium with trypsin. Supernatant samples were collected at indicated time points and PEDV titers were determined by serial dilutions of supernatant samples on Vero cells in medium with trypsin.[60] Co-expression of SAM vaccine and PEDV CV777 was examined by immunofluorescence staining using mouse monoclonal anti-PEDV spike (1:50, Friedrich Loeffler Institute) and goat polyclonal anti-mouse-Alexa Fluor 488 antibody (1:2,000, Invitrogen) as described.[85]

Coronavirus growth kinetics

PEDV CV777 and PEDV DR13 growth kinetics were determined by infection (0.1 $TCID_{50}$/cell) on Vero cells in the presence or absence of 10 μg/mL trypsin-EDTA (Gibco). One hour post infection, the infection fluid was removed, cell monolayers were washed with PBS, and fresh medium with or without trypsin was added. Viral titers were determined from supernatant samples by serial dilution on Vero cells in medium with trypsin.

Cell-based coronavirus recombination detection assay

RNA recombination events between SAM vaccine and PEDV CV777 were evaluated by serial passages of supernatant samples collected 72 h post transfection/infection. Samples were incubated for 3–4 days on Vero cells in the presence of absence of trypsin, passaged to fresh cell monolayers, and screened for CPE by eye using light inverted microscope. The sensitivity of the assay was illustrated by using serial dilutions of PEDV DR13 (Figure S9D).

DATA AND CODE AVAILABILITY

All data is included in the manuscript, in the databases mentioned in the materials and methods, and in the supplemental material. The sequencing files for chimeric viruses and mouse work have been submitted to the NCBI SRA PRJNA981649.

SUPPLEMENTAL INFORMATION

Supplemental information can be found online at https://doi.org/10.1016/j.ymthe.2024.06.019.

ACKNOWLEDGMENTS

We thank the TTW RepliSAFE (project 15791) user committee members for their continuous support, suggestions, and insightful discussions. We thank Prof. Dr. Roy Hall (University of Queensland, Brisbane, Australia), Prof. Dr. Michael Diamond (Washington University, USA), and Dr. Byron Martina (Erasmus Medical Center, the Netherlands) for providing alphavirus stocks. We thank Dr. Berend-Jan Bosch (Utrecht University, the Netherlands) for providing PEDV CV777 and PEDV DR13, and the defective PEDV DR13 construct. We thank Prof. Dr. Toos Daemen (University Medical Center Groningen, the Netherlands) for sharing detailed VRP production protocols. We also thank Marleen Henkens, Dr. Julian Bakker, Tessa Visser, and Dr. Athos Oliveira (Wageningen University and Research, the Netherlands) for their contribution to the alphavirus growth curves on the ΔG3BP cells. We thank Dr. Itaru Anraku (QIMR Berghofer) for managing the PC3 facility, Dr. Viviana Lutzky

(QIMR Berghofer) for help with proof reading, and the animal house staff at QIMR Berghofer MRI.
This project (TTW RepliSAFE, 15791) was funded by the research program "Toward Modernization of Biotechnology and Safety" of the Dutch Research Council (Domain Applied and Engineering Sciences), commissioned by the Dutch Ministry of Infrastructure and Water Management (I&W). A.S. was supported by an Investigator grant awarded to from the National Health and Medical Research Council of Australia (APP1173880).

AUTHOR CONTRIBUTIONS

G.P.P. conceived of the work. M.A.L. developed the G3BP knockout cells under the supervision of F.J.M.v.K. The *in vitro* experiments were performed by T.A.H.H., C.G., and S.R.A., and the resulting data were analyzed by T.A.H.H. under supervision of G.P.P. and M.M.v.O. Mouse work was conducted by T.A.H.H., W.N., B.T., and K.Y., with D.J.R. and A.S. who supervised the work and obtained the regulatory approvals. C.R.B. and T.D undertook the bioinformatic analyses. G.P.P. and A.S. obtained the funding. T.A.H.H., A.S., and G.P.P. wrote the manuscript. All authors reviewed the manuscript.

DECLARATION OF INTERESTS

The user committee for the RepliSAFE project included members from MSD Animal Health. MSD Animal Health provided TC-83 replicons and antibodies but otherwise provided no other resources or funding, had no input into the manuscript nor the decision to publish.

REFERENCES

1. Rappaport, A.R., Hong, S.J., Scallan, C.D., Gitlin, L., Akoopie, A., Boucher, G.R., Egorova, M., Espinosa, J.A., Fidanza, M., Kachura, M.A., et al. (2022). Low-dose self-amplifying mRNA COVID-19 vaccine drives strong protective immunity in non-human primates against SARS-CoV-2 infection. Nat. Commun. *13*, 3289. https://doi.org/10.1038/s41467-022-31005-z.

2. Szubert, A.J., Pollock, K.M., Cheeseman, H.M., Alagaratnam, J., Bern, H., Bird, O., Boffito, M., Byrne, R., Cole, T., Cosgrove, C.A., et al. (2023). COVAC1 phase 2a expanded safety and immunogenicity study of a self-amplifying RNA vaccine against SARS-CoV-2. EClinicalMedicine *56*, 101823. https://doi.org/10.1016/j.eclinm.2022.101823.

3. Bloom, K., van den Berg, F., and Arbuthnot, P. (2021). Self-amplifying RNA vaccines for infectious diseases. Gene Ther. *28*, 117–129. https://doi.org/10.1038/s41434-020-00204-y.

4. Schmidt, C., and Schnierle, B.S. (2023). Self-amplifying RNA vaccine candidates: alternative platforms for mRNA vaccine development. Pathogens *12*, 138. https://doi.org/10.3390/pathogens12010138.

5. Comes, J.D.G., Pijlman, G.P., and Hick, T.A.H. (2023). Rise of the RNA machines – self-amplification in mRNA vaccine design. Trends Biotechnol. *41*, 1417–1429. https://doi.org/10.1016/j.tibtech.2023.05.007.

6. Canadian Centre for Veterinary Biologics (2014). Environmental assessment for the emergency use of Harrisvaccines' unlicensed porcine epidemic diarrhea vaccine. iPED+. https://inspection.canada.ca/animal-health/veterinary-biologics/environmental-assessments/iped-vaccine/eng/1467040659842/1467040717031.

7. United States Department of Agriculture. Center for veterinary biologics notice No 17-01. (https://www.aphis.usda.gov/animal_health/vet_biologics/publications/notice_17_01.pdf).

8. Sawattrakool, K., Stott, C.J., Bandalaria-Marca, R.D., Srijangwad, A., Palabrica, D.J., and Nilubol, D. (2020). Field trials evaluating the efficacy of porcine epidemic diarrhea vaccine, RNA (Harrisvaccine) in the Philippines. Trop. Anim. Health Prod. *52*, 2743–2747. https://doi.org/10.1007/s11250-020-02270-1.

9. United States Department of Agriculture (2021). Veterinary biologics 165A-9PP000. https://www.aphis.usda.gov/aphis/ourfocus/animalhealth/veterinary-biologics/product-summaries/vet-label-data/98af0915-c6c9-481c-9e03-e11a6d52daff.

10. Gupta, S.L., Goswami, S., Anand, A., Naman, N., Kumari, P., Sharma, P., and Jaiswal, R.K. (2023). An assessment of the strategy and status of COVID-19 vaccination in India. Immunol. Res. *71*, 565–577. https://doi.org/10.1007/s12026-023-09373-5.

11. Gennova. Lyophilized mRNA vaccine for Injection (https://cdsco.gov.in/opencms/resources/UploadCDSCOWeb/2018/UploadSmPC/4.%20GEMCOVAC%20mRNA%20vaccine%20of%20Gennova_SmPC,%20factsheet%20&%20PI.pdf).

12. Central Drugs Standard Control Organization (2022). COVID-19 vaccines approved for primary vaccination series for restricted use in emergency situation in the country. https://cdsco.gov.in/opencms/opencms/system/modules/CDSCO.WEB/elements/download_file_division.jsp?num_id=OTA4MQ==.

13. Dolgin, E. (2023). Self-copying RNA vaccine wins first full approval: what's next? Nature.

14. Morse, M.A., Crosby, E.J., Force, J., Osada, T., Hobeika, A.C., Hartman, Z.C., Berglund, P., Smith, J., and Lyerly, H.K. (2023). Clinical trials of self-replicating RNA-based cancer vaccines. Cancer Gene Ther. *30*, 803–811. https://doi.org/10.1038/s41417-023-00587-1.

15. Pittman, P.R., Makuch, R.S., Mangiafico, J.A., Cannon, T.L., Gibbs, P.H., and Peters, C.J. (1996). Long-term duration of detectable neutralizing antibodies after administration of live-attenuated VEE vaccine and following booster vaccination with inactivated VEE vaccine. Vaccine *14*, 337–343. https://doi.org/10.1016/0264-410x(95)00168-z.

16. U.S. Army Medical Materiel Development Activity (2023). Special Immunizations Program. https://usammda.health.mil/index.cfm/fhp/immunizations_program.

17. México, C.d. (2018). EQUIVAC TC-83.

18. Ding, M.X., and Schlesinger, M.J. (1989). Evidence that Sindbis virus NSP2 is an autoprotease which processes the virus nonstructural polyprotein. Virology *171*, 280–284. https://doi.org/10.1016/0042-6822(89)90539-4.

19. Strauss, J.H., and Strauss, E.G. (1994). The alphaviruses: gene expression, replication, and evolution. Microbiol. Rev. *58*, 491–562. https://doi.org/10.1128/mr.58.3.491-562.1994.

20. Shirako, Y., and Strauss, J.H. (1994). Regulation of Sindbis virus RNA replication: uncleaved P123 and nsP4 function in minus-strand RNA synthesis, whereas cleaved products from P123 are required for efficient plus-strand RNA synthesis. J. Virol. *68*, 1874–1885. https://doi.org/10.1128/jvi.68.3.1874-1885.1994.

21. Lemm, J.A., Rümenapf, T., Strauss, E.G., Strauss, J.H., and Rice, C.M. (1994). Polypeptide requirements for assembly of functional Sindbis virus replication complexes: a model for the temporal regulation of minus- and plus-strand RNA synthesis. EMBO J. *13*, 2925–2934. https://doi.org/10.1002/j.1460-2075.1994.tb06587.x.

22. Wielgosz, M.M., Raju, R., and Huang, H.V. (2001). Sequence requirements for Sindbis virus subgenomic mRNA promoter function in cultured cells. J. Virol. *75*, 3509–3519. https://doi.org/10.1128/JVI.75.8.3509-3519.2001.

23. Kamrud, K.I., Alterson, K., Custer, M., Dudek, J., Goodman, C., Owens, G., and Smith, J.F. (2010). Development and characterization of promoterless helper RNAs for the production of alphavirus replicon particle. J. Gen. Virol. *91*, 1723–1727. https://doi.org/10.1099/vir.0.020081-0.

24. Hahn, C.S., Lustig, S., Strauss, E.G., and Strauss, J.H. (1988). Western equine encephalitis virus is a recombinant virus. Proc. Natl. Acad. Sci. USA *85*, 5997–6001. https://doi.org/10.1073/pnas.85.16.5997.

25. Mavian, C., Rife, B.D., Dollar, J.J., Cella, E., Ciccozzi, M., Prosperi, M.C.F., Lednicky, J., Morris, J.G., Capua, I., and Salemi, M. (2017). Emergence of recombinant Mayaro virus strains from the Amazon basin. Sci. Rep. *7*, 8718. https://doi.org/10.1038/s41598-017-07152-5.

26. Casal, P.E., Chouhy, D., Bolatti, E.M., Perez, G.R., Stella, E.J., and Giri, A.A. (2015). Evidence for homologous recombination in Chikungunya Virus. Mol. Phylogenet. Evol. *85*, 68–75. https://doi.org/10.1016/j.ympev.2015.01.016.

27. Hajjou, M., Hill, K.R., Subramaniam, S.V., Hu, J.Y., and Raju, R. (1996). Nonhomologous RNA-RNA recombination events at the 3' nontranslated region of the Sindbis virus genome: hot spots and utilization of nonviral sequences. J. Virol. *70*, 5153–5164. https://doi.org/10.1128/JVI.70.8.5153-5164.1996.

28. Hill, K.R., Hajjou, M., Hu, J.Y., and Raju, R. (1997). RNA-RNA recombination in Sindbis virus: roles of the 3' conserved motif, poly(A) tail, and nonviral sequences of template RNAs in polymerase recognition and template switching. J. Virol. *71*, 2693–2704. https://doi.org/10.1128/JVI.71.4.2693-2704.1997.

29. Petterson, E., Guo, T.C., Evensen, Ø., and Mikalsen, A.B. (2016). Experimental piscine alphavirus RNA recombination in vivo yields both viable virus and defective viral RNA. Sci. Rep. *6*, 36317. https://doi.org/10.1038/srep36317.

30. Filomatori, C.V., Bardossy, E.S., Merwaiss, F., Suzuki, Y., Henrion, A., Saleh, M.C., and Alvarez, D.E. (2019). RNA recombination at Chikungunya virus 3'UTR as an evolutionary mechanism that provides adaptability. Plos Pathog. *15*, e1007706. https://doi.org/10.1371/journal.ppat.1007706.

31. Langsjoen, R.M., Muruato, A.E., Kunkel, S.R., Jaworski, E., and Routh, A. (2020). Differential Alphavirus Defective RNA Diversity between Intracellular and Extracellular Compartments Is Driven by Subgenomic Recombination Events. mBio *11*, e00731-20. https://doi.org/10.1128/mBio.00731-20.

32. Lello, L.S., Utt, A., Bartholomeeusen, K., Wang, S., Rausalu, K., Kendall, C., Coppens, S., Fragkoudis, R., Tuplin, A., Alphey, L., et al. (2020). Cross-utilisation of template RNAs by alphavirus replicases. Plos Pathog. *16*, e1008825. https://doi.org/10.1371/journal.ppat.1008825.

33. Kautz, T.F., Jaworski, E., Routh, A., and Forrester, N.L. (2020). A Low Fidelity Virus Shows Increased Recombination during the Removal of an Alphavirus Reporter Gene. Viruses *12*, 660. https://doi.org/10.3390/v12060660.

34. Smerdou, C., and Liljeström, P. (1999). Two-helper RNA system for production of recombinant Semliki forest virus particles. J. Virol. *73*, 1092–1098. https://doi.org/10.1128/JVI.73.2.1092-1098.1999.

35. Condit, R.C., Williamson, A.L., Sheets, R., Seligman, S.J., Monath, T.P., Excler, J.L., Gurwith, M., Bok, K., Robertson, J.S., Kim, D., et al. (2016). Unique safety issues associated with virus-vectored vaccines: Potential for and theoretical consequences of recombination with wild type virus strains. Vaccine *34*, 6610–6616. https://doi.org/10.1016/j.vaccine.2016.04.060.

36. Suhrbier, A., Jaffar-Bandjee, M.C., and Gasque, P. (2012). Arthritogenic alphaviruses -an overview. Nat. Rev. Rheumatol. *8*, 420–429. https://doi.org/10.1038/nrrheum.2012.64.

37. Singer, Z.S., Ambrose, P.M., Danino, T., and Rice, C.M. (2021). Quantitative measurements of early alphaviral replication dynamics in single cells reveals the basis for superinfection exclusion. Cell Syst. *12*, 210–219.e3. https://doi.org/10.1016/j.cels.2020.12.005.

38. Boussier, J., Levi, L., Weger-Lucarelli, J., Poirier, E.Z., Vignuzzi, M., and Albert, M.L. (2020). Chikungunya virus superinfection exclusion is mediated by a block in viral replication and does not rely on non-structural protein 2. PloS one *15*, e0241592. https://doi.org/10.1371/journal.pone.0241592.

39. Comes, J.D.G., Doets, K., Zegers, T., Kessler, M., Slits, I., Ballesteros, N.A., van de Weem, N.M.P., Pouwels, H., van Oers, M.M., van Hulten, M.C.W., et al. (2024). Evaluation of bird-adapted self-amplifying mRNA vaccine formulations in chickens. Vaccine *42*, 2895–2908. https://doi.org/10.1016/j.vaccine.2024.03.032.

40. Hick, T., Zotler, T., Bosveld, D., Geertsema, C., Oers, M.v., and Pijlman, G. (2024). Venezuelan equine encephalitis virus non-structural protein 3 dictates superinfection exclusion in mammalian cells. Res. Square. https://doi.org/10.21203/rs.3.rs-4162845/v1.

41. Comas-Garcia, M. (2019). Packaging of genomic RNA in positive-sense single-stranded RNA viruses: A complex story. Viruses *11*, 253. https://doi.org/10.3390/v11030253.

42. Kim, D.Y., Firth, A.E., Atasheva, S., Frolova, E.I., and Frolov, I. (2011). Conservation of a packaging signal and the viral genome RNA packaging mechanism in alphavirus evolution. J. Virol. *85*, 8022–8036. https://doi.org/10.1128/jvi.00644-11.

43. Fros, J.J., Domeradzka, N.E., Baggen, J., Geertsema, C., Flipse, J., Vlak, J.M., and Pijlman, G.P. (2012). Chikungunya virus nsP3 blocks stress granule assembly by recruitment of G3BP into cytoplasmic foci. J. Virol. *86*, 10873–10879. https://doi.org/10.1128/JVI.01506-12.

44. Scholte, F.E.M., Tas, A., Albulescu, I.C., Žusinaite, E., Merits, A., Snijder, E.J., and van Hemert, M.J. (2015). Stress granule components G3BP1 and G3BP2 play a proviral role early in Chikungunya virus replication. J. Virol. *89*, 4457–4469. https://doi.org/10.1128/JVI.03612-14.

45. Meshram, C.D., Agback, P., Shiliaev, N., Urakova, N., Mobley, J.A., Agback, T., Frolova, E.I., and Frolov, I. (2018). Multiple host factors interact with the hypervariable domain of chikungunya virus nsP3 and determine viral replication in cell-specific mode. J. Virol. *92*, e00838-18. https://doi.org/10.1128/JVI.00838-18.

46. Kim, D.Y., Reynaud, J.M., Rasalouskaya, A., Akhrymuk, I., Mobley, J.A., Frolov, I., and Frolova, E.I. (2016). New World and Old World alphaviruses have evolved to exploit different components of stress granules, FXR and G3BP proteins, for assembly of viral replication complexes. Plos Pathog. *12*, e1005810. https://doi.org/10.1371/journal.ppat.1005810.

47. MacDonald, G.H., and Johnston, R.E. (2000). Role of dendritic cell targeting in Venezuelan equine encephalitis virus pathogenesis. J. Virol. *74*, 914–922. https://doi.org/10.1128/jvi.74.2.914-922.2000.

48. Nishimoto, K.P., Laust, A.K., Wang, K., Kamrud, K.I., Hubby, B., Smith, J.F., and Nelson, E.L. (2007). Restricted and selective tropism of a Venezuelan equine encephalitis virus-derived replicon vector for human dendritic cells. Viral Immunol. *20*, 88–104. https://doi.org/10.1089/vim.2006.0090.

49. Tonkin, D.R., Whitmore, A., Johnston, R.E., and Barro, M. (2012). Infected dendritic cells are sufficient to mediate the adjuvant activity generated by Venezuelan equine encephalitis virus replicon particles. Vaccine *30*, 4532–4542. https://doi.org/10.1016/j.vaccine.2012.04.030.

50. Prow, N.A., Tang, B., Gardner, J., Le, T.T., Taylor, A., Poo, Y.S., Nakayama, E., Hirata, T.D.C., Nakaya, H.I., Slonchak, A., et al. (2017). Lower temperatures reduce type I interferon activity and promote alphaviral arthritis. Plos Pathog. *13*, e1006788. https://doi.org/10.1371/journal.ppat.1006788.

51. Bishop, C.R., Caten, F.T., Nakaya, H.I., and Suhrbier, A. (2022). Chikungunya patient transcriptional signatures faithfully recapitulated in a C57BL/6J mouse model. Front. Immunol. *13*, 1092370. https://doi.org/10.3389/fimmu.2022.1092370.

52. Nguyen, W., Nakayama, E., Yan, K., Tang, B., Le, T.T., Liu, L., Cooper, T.H., Hayball, J.D., Faddy, H.M., Warrilow, D., et al. (2020). Arthritogenic alphavirus vaccines: Serogrouping versus cross-protection in mouse models. Vaccines (Basel) *8*, 209. https://doi.org/10.3390/vaccines8020209.

53. Poo, Y.S., Rudd, P.A., Gardner, J., Wilson, J.A.C., Larcher, T., Colle, M.A., Le, T.T., Nakaya, H.I., Warrilow, D., Allcock, R., et al. (2014). Multiple immune factors are involved in controlling acute and chronic chikungunya virus infection. Plos Negl. Trop. Dis. *8*, e3354. https://doi.org/10.1371/journal.pntd.0003354.

54. Rudd, P.A., Wilson, J., Gardner, J., Larcher, T., Babarit, C., Le, T.T., Anraku, I., Kumagai, Y., Loo, Y.M., Gale, M., Jr., et al. (2012). Interferon response factors 3 and 7 protect against Chikungunya virus hemorrhagic fever and shock. J. Virol. *86*, 9888–9898. https://doi.org/10.1128/JVI.00956-12.

55. Gardner, J., Rudd, P.A., Prow, N.A., Belarbi, E., Roques, P., Larcher, T., Gresh, L., Balmaseda, A., Harris, E., Schroder, W.A., and Suhrbier, A. (2015). Infectious chikungunya virus in the saliva of mice, monkeys and humans. PloS one *10*, e0139481. https://doi.org/10.1371/journal.pone.0139481.

56. Yan, B., Chakravorty, S., Mirabelli, C., Wang, L., Trujillo-Ochoa, J.L., Chauss, D., Kumar, D., Lionakis, M.S., Olson, M.R., Wobus, C.E., et al. (2021). Host-virus chimeric events in SARS-CoV-2-infected cells are infrequent and artifactual. J. Virol. *95*, e0029421. https://doi.org/10.1128/JVI.00294-21.

57. Shang, G., Seed, C.R., Gahan, M.E., Rolph, M.S., and Mahalingam, S. (2012). Duration of Ross River viraemia in a mouse model–implications for transfusion transmission. Vox Sang. *102*, 185–192. https://doi.org/10.1111/j.1423-0410.2011.01536.x.

58. Focosi, D., and Maggi, F. (2022). Recombination in coronaviruses, with a focus on SARS-CoV-2. Viruses *14*, 1239. https://doi.org/10.3390/v14061239.

59. Tamura, T., Ito, J., Uriu, K., Zahradnik, J., Kida, I., Anraku, Y., Nasser, H., Shofa, M., Oda, Y., Lytras, S., et al. (2023). Virological characteristics of the SARS-CoV-2 XBB variant derived from recombination of two Omicron subvariants. Nat. Commun. *14*, 2800. https://doi.org/10.1038/s41467-023-38435-3.

60. Wicht, O., Li, W., Willems, L., Meuleman, T.J., Wubbolts, R.W., van Kuppeveld, F.J.M., Rottier, P.J.M., and Bosch, B.J. (2014). Proteolytic activation of the porcine epidemic diarrhea coronavirus spike fusion protein by trypsin in cell culture. J. Virol. *88*, 7952–7961. https://doi.org/10.1128/JVI.00297-14.

61. Li, W., Wicht, O., van Kuppeveld, F.J.M., He, Q., Rottier, P.J.M., and Bosch, B.J. (2015). A single point mutation creating a furin cleavage site in the spike protein

renders porcine epidemic diarrhea coronavirus trypsin independent for cell entry and fusion. J. Virol. *89*, 8077–8081. https://doi.org/10.1128/JVI.00356-15.

62. Kumanodmido, T., Wada, R., Kanemaru, T., Kamada, M., Hirasawa, K., and Akiyama, Y. (1988). Clinical and virological observations on swine experimentally infected with Getah virus. Vet. Microbiol. *16*, 295–301.

63. Pijlman, G.P., Suhrbier, A., and Khromykh, A.A. (2006). Kunjin virus replicons: an RNA-based, non-cytopathic viral vector system for protein production, vaccine and gene therapy applications. Expert Opin. Biol. Ther. *6*, 135–145. https://doi.org/10.1517/14712598.6.2.135.

64. Stokes, A., Pion, J., Binazon, O., Laffont, B., Bigras, M., Dubois, G., Blouin, K., Young, J.K., Ringenberg, M.A., Ben Abdeljelil, N., et al. (2020). Nonclinical safety assessment of repeated administration and biodistribution of a novel rabies self-amplifying mRNA vaccine in rats. Regul. Toxicol. Pharmacol. *113*, 104648. https://doi.org/10.1016/j.yrtph.2020.104648.

65. Kumar, R., Shrivastava, T., Samal, S., Ahmed, S., and Parray, H.A. (2020). Antibody-based therapeutic interventions: possible strategy to counter chikungunya viral infection. Appl. Microbiol. Biotechnol. *104*, 3209–3228. https://doi.org/10.1007/s00253-020-10437-x.

66. Wilson, J.A.C., Prow, N.A., Schroder, W.A., Ellis, J.J., Cumming, H.E., Gearing, L.J., Poo, Y.S., Taylor, A., Hertzog, P.J., Di Giallonardo, F., et al. (2017). RNA-Seq analysis of chikungunya virus infection and identification of granzyme A as a major promoter of arthritic inflammation. Plos Pathog. *13*, e1006155. https://doi.org/10.1371/journal.ppat.1006155.

67. Hugo, L.E., Prow, N.A., Tang, B., Devine, G., and Suhrbier, A. (2016). Chikungunya virus transmission between Aedes albopictus and laboratory mice. Parasit. Vectors *9*, 555. https://doi.org/10.1186/s13071-016-1838-1.

68. Sam, S.S., Mohamed-Romai-Noor, N.A., Teoh, B.T., Hamim, Z.R., Ng, H.Y., Abd-Jamil, J., Khor, C.S., Hassan, S.S., Ahmad, H., and AbuBakar, S. (2022). Group IV getah virus in Culex mosquitoes, Malaysia. Emerg. Infect. Dis. *28*, 475–477. https://doi.org/10.3201/eid2802.204887.

69. Franz, A.W.E., Kantor, A.M., Passarelli, A.L., and Clem, R.J. (2015). Tissue barriers to arbovirus infection in mosquitoes. Viruses *7*, 3741–3767. https://doi.org/10.3390/v7072795.

70. Suhrbier, A. (2019). Rheumatic manifestations of chikungunya: emerging concepts and interventions. Nat. Rev. Rheumatol. *15*, 597–611. https://doi.org/10.1038/s41584-019-0276-9.

71. Raju, R., Subramaniam, S.V., and Hajjou, M. (1995). Genesis of Sindbis virus by in vivo recombination of nonreplicative RNA precursors. J. Virol. *69*, 7391–7401.

72. Perri, S., Greer, C.E., Thudium, K., Doe, B., Legg, H., Liu, H., Romero, R.E., Tang, Z., Bin, Q., Dubensky, T.W., Jr., et al. (2003). An alphavirus replicon particle chimera derived from venezuelan equine encephalitis and sindbis viruses is a potent gene-based vaccine delivery vector. J. Virol. *77*, 10394–10403. https://doi.org/10.1128/jvi.77.19.10394-10403.2003.

73. Zhang, Y., Burke, C.W., Ryman, K.D., and Klimstra, W.B. (2007). Identification and characterization of interferon-induced proteins that inhibit alphavirus replication. J. Virol. *81*, 11246–11255. https://doi.org/10.1128/JVI.01282-07.

74. Frolov, I., Hardy, R., and Rice, C.M. (2001). Cis-acting RNA elements at the 5' end of Sindbis virus genome RNA regulate minus- and plus-strand RNA synthesis. RNA *7*, 1638–1651. https://doi.org/10.1017/s135583820101010x.

75. Ahola, T., McInerney, G., and Merits, A. (2021). Alphavirus RNA replication in vertebrate cells. Adv. Virus Res. *111*, 111–156. https://doi.org/10.1016/bs.aivir.2021.07.003.

76. Laurent, T., Kumar, P., Liese, S., Zare, F., Jonasson, M., Carlson, A., and Carlson, L.A. (2022). Architecture of the chikungunya virus replication organelle. Elife *11*, e83042. https://doi.org/10.7554/eLife.83042.

77. Mihelc, E.M., Baker, S.C., and Lanman, J.K. (2021). Coronavirus infection induces progressive restructuring of the endoplasmic reticulum involving the formation and degradation of double membrane vesicles. Virology *556*, 9–22. https://doi.org/10.1016/j.virol.2020.12.007.

78. Mironov, A.A., Savin, M.A., and Beznoussenko, G.V. (2023). COVID-19 Biogenesis and Intracellular Transport. Int. J. Mol. Sci. *24*, 4523. https://doi.org/10.3390/ijms24054523.

79. Bernardo, P., Golden, M., Akram, M., Roumagnac, P., Naimuddin, Nadarajan, N., Nadarajan, N., Fernandez, E., Granier, M., Rebelo, A.G., et al. (2013). Identification and characterisation of a highly divergent geminivirus: Evolutionary and taxonomic implications. Virus Res. *177*, 35–45.

80. Di Mattia, J., Ryckebusch, F., Vernerey, M.S., Pirolles, E., Sauvion, N., Peterschmitt, M., Zeddam, J.L., and Blanc, S. (2020). Co-Acquired Nanovirus and Geminivirus Exhibit a Contrasted Localization within Their Common Aphid Vector. Viruses *12*, 299.

81. Huang, C., Liu, W.J., Xu, W., Jin, T., Zhao, Y., Song, J., Shi, Y., Ji, W., Jia, H., Zhou, Y., et al. (2016). A bat-derived putative cross-family recombinant coronavirus with a reovirus gene. Plos Pathog. *12*, e1005883.

82. Zhai, X., Li, X., Veit, M., Wang, N., Wang, Y., Merits, A., Jiang, Z., Qin, Y., Zhang, X., Qi, K., et al. (2024). LDLR is used as a cell entry receptor by multiple alphaviruses. Nat. Commun. *15*, 622.

83. Amarilla, A.A., Sng, J.D.J., Parry, R., Deerain, J.M., Potter, J.R., Setoh, Y.X., Rawle, D.J., Le, T.T., Modhiran, N., Wang, X., et al. (2021). A versatile reverse genetics platform for SARS-CoV-2 and other positive-strand RNA viruses. Nat. Commun. *12*, 3431. https://doi.org/10.1038/s41467-021-23779-5.

84. Visser, L.J., Langereis, M.A., Rabouw, H.H., Wahedi, M., Muntjewerff, E.M., de Groot, R.J., and van Kuppeveld, F.J.M. (2019). Essential role of enterovirus 2A protease in counteracting stress granule formation and the induction of type I interferon. J. Virol. *93*, e00222-19. https://doi.org/10.1128/JVI.00222-19.

85. Göertz, G.P., Vogels, C.B.F., Geertsema, C., Koenraadt, C.J.M., and Pijlman, G.P. (2017). Mosquito co-infection with Zika and chikungunya virus allows simultaneous transmission without affecting vector competence of Aedes aegypti. Plos Negl. Trop. Dis. *11*, e0005654. https://doi.org/10.1371/journal.pntd.0005654.

86. Swann, J.B., Hayakawa, Y., Zerafa, N., Sheehan, K.C.F., Scott, B., Schreiber, R.D., Hertzog, P., and Smyth, M.J. (2007). Type I IFN contributes to NK cell homeostasis, activation, and antitumor function. J. Immunol. *178*, 7540–7549. https://doi.org/10.4049/jimmunol.178.12.7540.

87. Rawle, D.J., Nguyen, W., Dumenil, T., Parry, R., Warrilow, D., Tang, B., Le, T.T., Slonchak, A., Khromykh, A.A., Lutzky, V.P., et al. (2020). Sequencing of historical isolates, K-mer mining and high serological cross-reactivity with Ross River virus argue against the presence of getah virus in Australia. Pathogens *9*, 848. https://doi.org/10.3390/pathogens9100848.

88. Rawle, D.J., Le, T.T., Dumenil, T., Bishop, C., Yan, K., Nakayama, E., Bird, P.I., and Suhrbier, A. (2022). Widespread discrepancy in Nnt genotypes and genetic backgrounds complicates granzyme A and other knockout mouse studies. eLife *11*, e70207. https://doi.org/10.7554/eLife.70207.

89. Bishop, C.R., Dumenil, T., Rawle, D.J., Le, T.T., Yan, K., Tang, B., Hartel, G., and Suhrbier, A. (2022). Mouse models of COVID-19 recapitulate inflammatory pathways rather than gene expression. Plos Pathog. *18*, e1010867. https://doi.org/10.1371/journal.ppat.1010867.

90. Dumenil, T., Le, T.T., Rawle, D.J., Yan, K., Tang, B., Nguyen, W., Bishop, C., and Suhrbier, A. (2023). Warmer ambient air temperatures reduce nasal turbinate and brain infection, but increase lung inflammation in the K18-hACE2 mouse model of COVID-19. Sci. Total Environ. *859*, 160163. https://doi.org/10.1016/j.scitotenv.2022.160163.

91. Yan, K., Vet, L.J., Tang, B., Hobson-Peters, J., Rawle, D.J., Le, T.T., Larcher, T., Hall, R.A., and Suhrbier, A. (2020). A yellow fever virus 17D infection and disease mouse model used to evaluate a chimeric Binjari-yellow fever virus vaccine. Vaccines (Basel) *8*, 368. https://doi.org/10.3390/vaccines8030368.

92. Komdeur, F.L., Singh, A., Van De Wall, S., Meulenberg, J.J.M., Boerma, A., Hoogeboom, B.N., Paijens, S.T., Oyarce, C., De Bruyn, M., Schuuring, E., et al. (2021). First-in-human phase I clinical trial of an SFV-based RNA replicon cancer vaccine against HPV-induced cancers. Mol. Ther. *29*, 611–625. https://doi.org/10.1016/j.ymthe.2020.11.002.

93. Morse, M.A., Hobeika, A., Gwin, W., Osada, T., Gelles, J., Rushing, C., Niedzwiecki, D., and Lyerly, H.K. (2015). Phase I study of alphaviral vector (AVX701) in colorectal cancer patients: Comparison of immune responses in stage III and stage IV patients. J. Immunother. Cancer *3*, P4444. https://doi.org/10.1186/2051-1426-3-S2-P444.

94. Bernstein, D.I., Reap, E.A., Katen, K., Watson, A., Smith, K., Norberg, P., Olmsted, R.A., Hoeper, A., Morris, J., Negri, S., et al. (2009). Randomized, double-blind,

Phase 1 trial of an alphavirus replicon vaccine for cytomegalovirus in CMV seronegative adult volunteers. Vaccine *28*, 484–493. https://doi.org/10.1016/j.vaccine.2009.09.135.

95. Wecker, M., Gilbert, P., Russell, N., Hural, J., Allen, M., Pensiero, M., Chulay, J., Chiu, Y.-L., Abdool Karim, S.S., Burke, D.S., et al. (2012). Phase I safety and immunogenicity evaluations of an alphavirus replicon HIV-1 subtype C gag vaccine in healthy HIV-1-uninfected adults. Clin. Vaccin. Immunol. *19*, 1651–1660. https://doi.org/10.1128/cvi.00258-12.

96. Palmer, C.D., Rappaport, A.R., Davis, M.J., Hart, M.G., Scallan, C.D., Hong, S.-J., Gitlin, L., Kraemer, L.D., Kounlavouth, S., Yang, A., et al. (2022). Individualized, heterologous chimpanzee adenovirus and self-amplifying mRNA neoantigen vaccine for advanced metastatic solid tumors: phase 1 trial interim results. Nat. Med. *28*, 1619–1629. https://doi.org/10.1038/s41591-022-01937-6.

97. Elliott, S.L., Suhrbier, A., Miles, J.J., Lawrence, G., Pye, S.J., Le, T.T., Rosenstengel, A., Nguyen, T., Allworth, A., Burrows, S.R., et al. (2008). Phase I trial of a CD8+ T-cell peptide epitope-based vaccine for infectious mononucleosis. J. Virol. *82*, 1448–1457. https://doi.org/10.1128/JVI.01409-07.

98. Pollock, K.M., Cheeseman, H.M., Szubert, A.J., Libri, V., Boffito, M., Owen, D., Bern, H., O'Hara, J., McFarlane, L.R., Lemm, N.M., et al. (2022). Safety and immunogenicity of a self-amplifying RNA vaccine against COVID-19: COVAC1, a phase I, dose-ranging trial. EClinicalMedicine *44*, 101262. https://doi.org/10.1016/j.eclinm.2021.101262.

99. Maruggi, G., Mallett, C.P., Westerbeck, J.W., Chen, T., Lofano, G., Friedrich, K., Qu, L., Sun, J.T., McAuliffe, J., Kanitkar, A., et al. (2022). A self-amplifying mRNA SARS-CoV-2 vaccine candidate induces safe and robust protective immunity in preclinical models. Mol. Ther. *30*, 1897–1912. https://doi.org/10.1016/j.ymthe.2022.01.001.

YMTHE, Volume *32*

Supplemental Information

Safety concern of recombination between self-amplifying mRNA vaccines and viruses is mitigated *in vivo*

Tessy A.H. Hick, Corinne Geertsema, Wilson Nguyen, Cameron R. Bishop, Linda van Oosten, Sandra R. Abbo, Troy Dumenil, Frank J.M. van Kuppeveld, Martijn A. Langereis, Daniel J. Rawle, Bing Tang, Kexin Yan, Monique M. van Oers, Andreas Suhrbier, and Gorben P. Pijlman

Supplemental Tables and Figures

Table S1. RNA-Seq read pairs derived from feet. Polyadenylated positive strand RNA sequences of GETV, SAM vaccine and mouse present in RNA isolated from feet identified by RNA-seq. Chimeric read-pairs identified from all mouse foot RNA-Seq data. Chimeric cDNA species likely arise as artefacts due to random template switching during reverse-transcription (RT)[1] (see Supplemental Fig. 6 and 7).

Strain	Time (dpi)	Sample	Proper read pairs				Chimeric read pairs	
			Total	GETV	SAM	Mouse	GETV/ SAM	Mouse
C57BL/6J	2	CCg24	16,496,555	357	550	16,094,607	0	661
		Cg25	17,444,881	274	516	17,010,685	0	542
		Cg26	15,482,350	272	674	14,938,719	0	535
	3	Cg21	16,509,615	438	78	16,195,705	0	498
		Cg22	15,675,118	2,993	4	14,895,533	0	303
		Cg23	16,223,836	155	25	15,884,778	0	605
Ifnar$^{-/-}$	2	Cg51	16,047,840	421,495	5,116	15,071,584	1	438
		Cg52	17,425,852	462,229	10,783	16,204,692	2	240
		Cg61	15,998,134	347,707	5,836	15,130,673	0	435
	3	Cg21	18,994,287	1,655,929	5,293	16,886,302	0	516
		Cg41	17,238,761	2,142,702	5,556	14,694,258	1	467
		Cg42	15,706,105	882,896	2,818	14,422,143	0	498
	5	Cg11	21,969,798	3,583,158	3,925	17,884,208	0	1110
		Cg31	16,841,127	2,722,173	3,959	13,673,336	0	944
Rag1$^{-/-}$	2	Cg83	18,491,093	94	45	18,183,205	0	391
		Cg84	18,007,132	141	133	16,885,390	0	48
		Cg85	19,604,811	431	133	18,696,171	0	114
	3	Cg81	18,108,538	340	21	17,150,222	0	244
		Cg82	14,059,628	708	5	13,581,597	0	469
		Cg86	20,155,651	210	73	19,724,814	0	698
	14	Cg74	16,923,637	2,710	7	16,520,045	0	556
		Cg75	16,244,992	2,907,751	3,866	12,818,883	1	844
		Cg76	17,387,562	421	6	16,930,047	0	483
Total			**397,037,303**	**15,135,584**	**49,422**	**369,477,597**	**5**	**11,639**

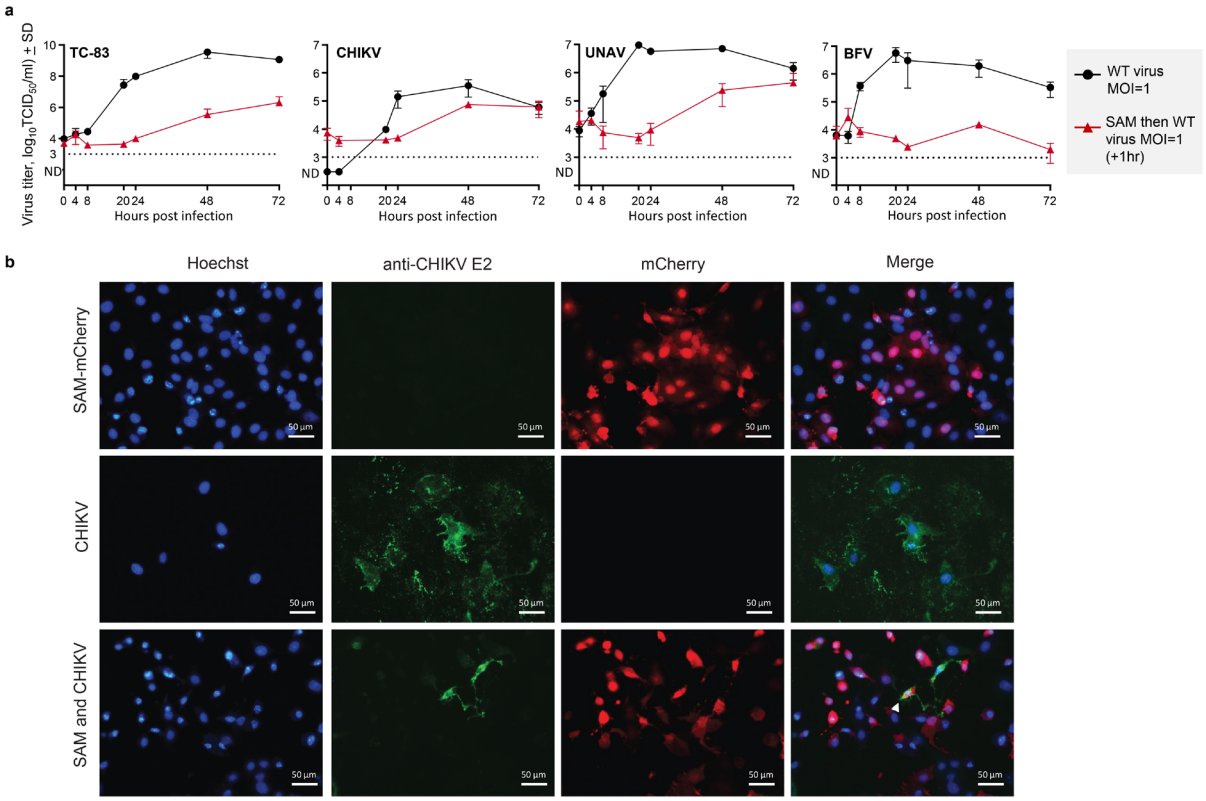

Figure S1. Superinfection exclusion and co-expression. Vero cells were transduced with SAM (10 VRPs/cell) and infected with WT alphaviruses (MOI=1 $TCID_{50}$/cell) with a 1 hour delay (n=2). Supernatant fractions were collected and titrated to determine WT alphavirus growth kinetics by serial dilutions on Vero cells (detection limit 3 $log_{10}TCID_{50}$/ml). **b**, Fluorescence microscopy of co-transduced/infected Vero cell; cell nuclei stained with Hoechst, WT alphavirus (CHIKV) stained with rabbit anti-CHIKV E2 (1:5000), and SAM vaccine mCherry expression.

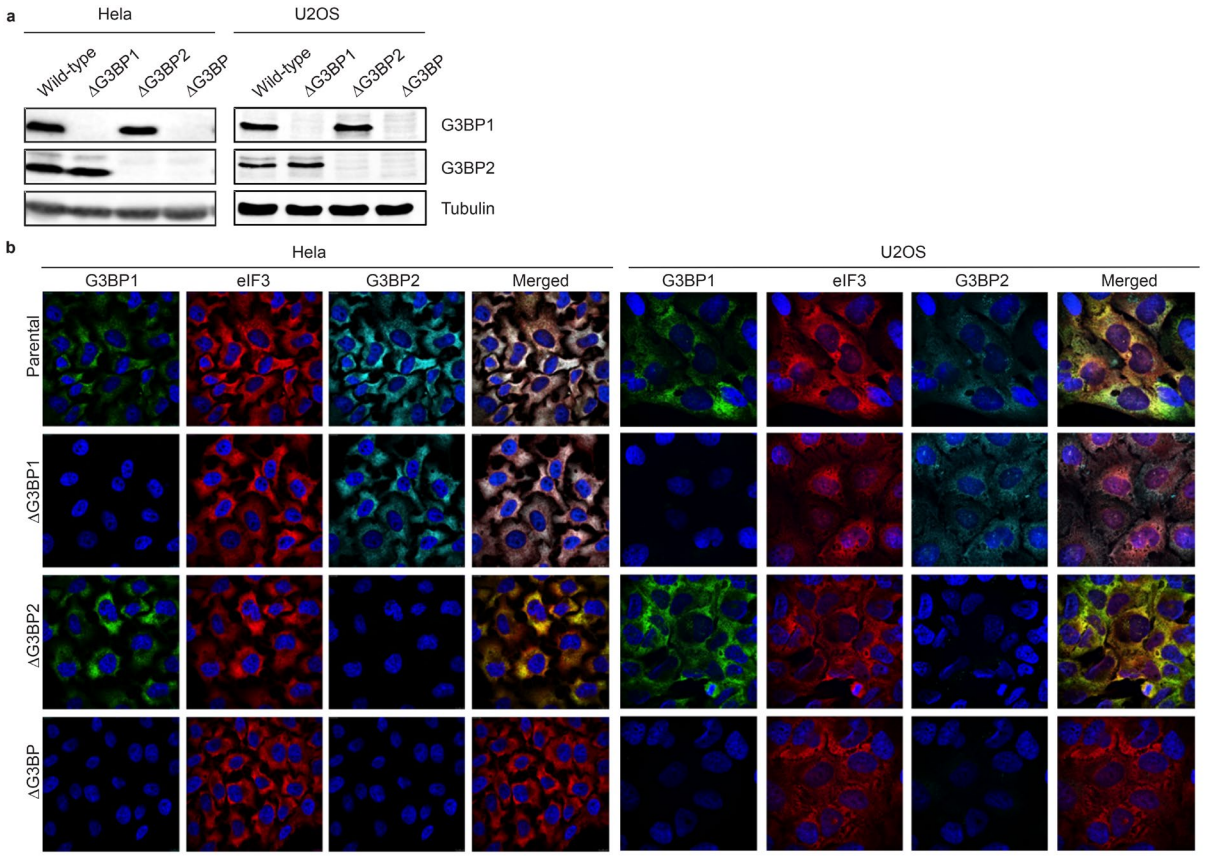

Figure S2. Hela and U2OS ΔG3BP cell lines. Hela and U2OS G3BP deficient cells (ΔG3BP) were generated using CRISPR-Cas9 technology to delete expression of G3BP1 (ΔG3BP1), G3BP2 (ΔG3BP2), or both (ΔG3BP) as described[2]. **a** Western blot showing loss of G3BP in Hela and U2OS cells. **b** Immunofluorescence assay using mouse anti-G3BP (BD biosciences, 1:2000), rabbit anti-G3BP2 (1:2000, Bethyl), anti-tubulin (1:5000, Sigma-Aldrich), and anti-eIF2 (stress granular identification factor, 1:200, SantaCruz) antibodies.

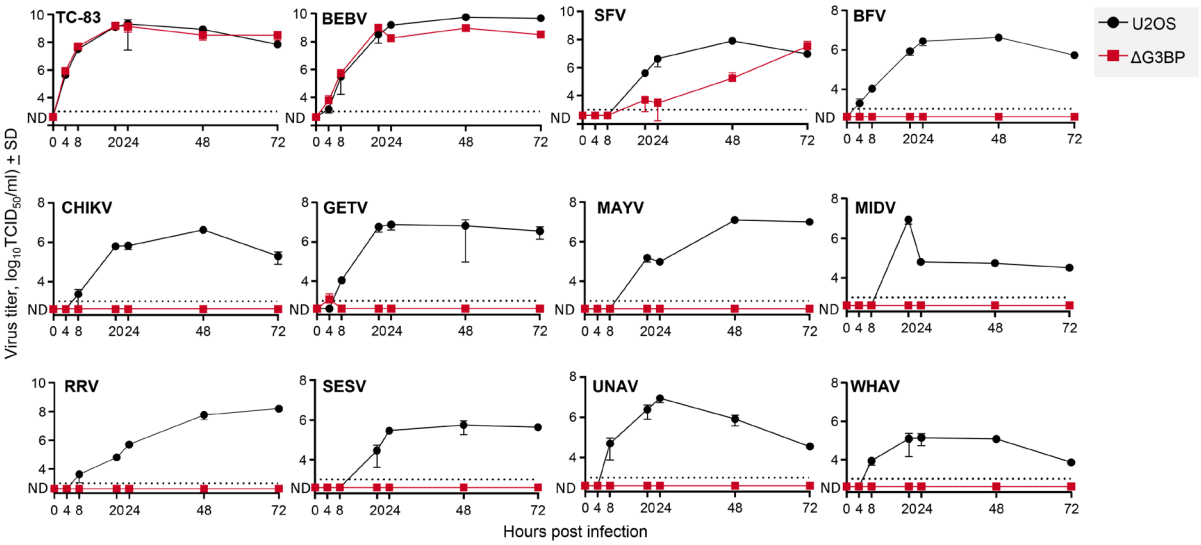

Figure S3. Alphavirus replication kinetics on U2OS ΔG3BP cells. U2OS and U2OS ΔG3BP cells were infected with various alphaviruses (0.1 $TCID_{50}$/cell, n=2). Supernatant fractions were collected and titrated to determine alphavirus growth kinetics (detection limit 3 $log_{10}TCID_{50}$/ml).Venezuelan equine encephalitis virus TC-83 (TC-83), Bebaru virus (BEBV), and Semliki Forest virus (SFV) demonstrated to replicate independently of G3BP, whereas Barmah Forest virus (BFV), chikungunya virus (CHIKV), getah virus (GETV), Mayaro virus (MAYV), Middelburg virus (MIDV), Ross River virus (RRV), southern elephant seal virus (SESV), Una virus (UNAV), and Whataroa virus (WHAV) required the presence of G3BP for efficient virus replication.

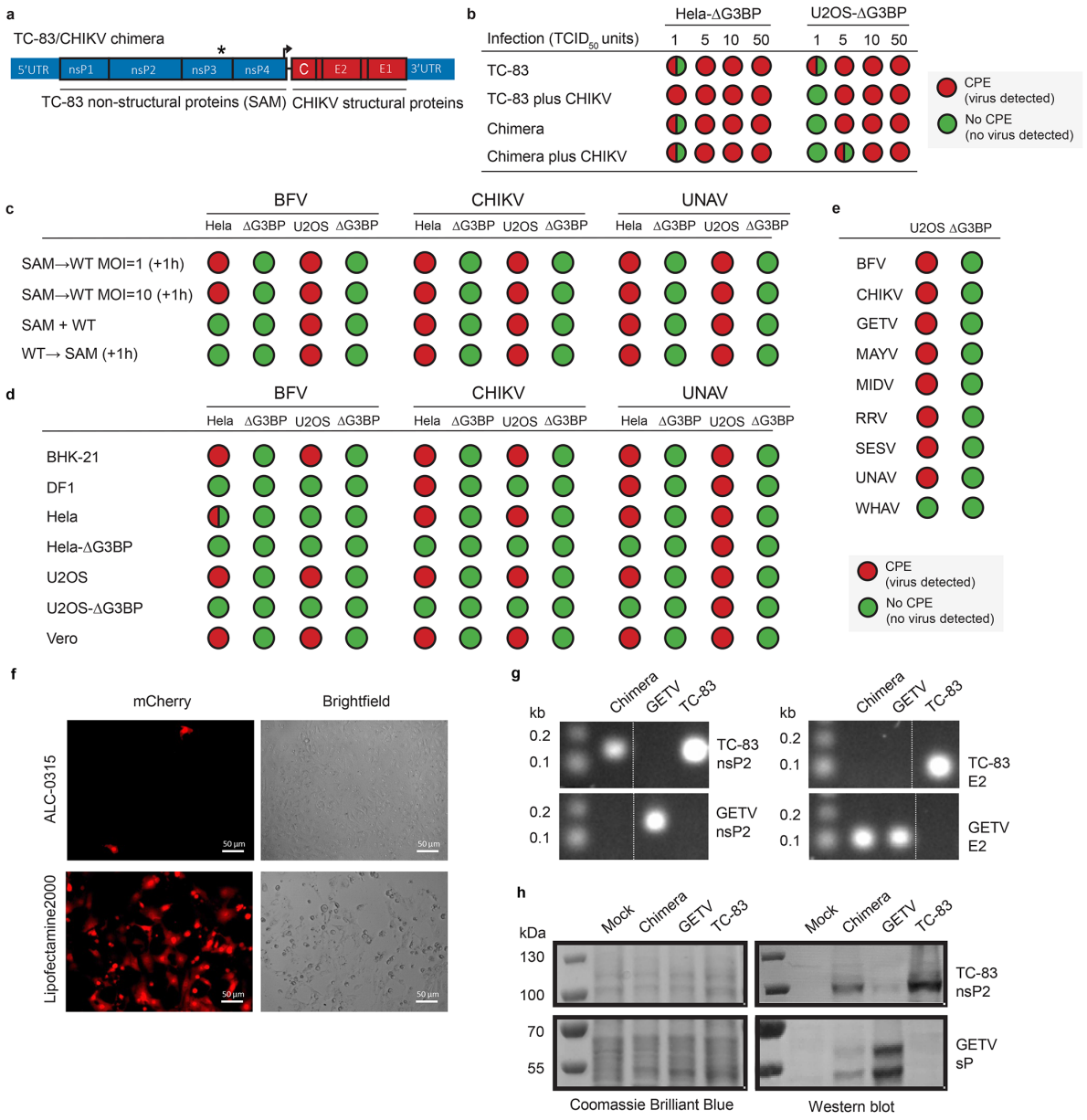

Figure S4. Alphavirus recombination detection assay using ΔG3BP cells. a, An alphavirus chimera was constructed, that encoded the nsPs of TC-83 (SAM) and the structural proteins of CHIKV S27, by cloning the latter into the multiple cloning site of the SAM plasmid. The hypervariable domain of nsP3 (indicated by asterisk) confers G3BP independent replication capacity. This infectious clone was recovered after lipofectamine-mediated transfection of Vero cells. **b**, The TC-83/CHIKV chimera and TC-83 were able to replicate and induce CPE in 10^5 ΔG3BP cells within four serial passages even at low MOI and in the presence of an excess of G3BP-dependent CHIKV ($5x10^5$ $TCID_{50}$), illustrating the assay's sensitivity and suitability. **c**, Supernatants from Vero cells transduced with a SAM vaccine encoding mCherry (10 VRPs/cell) and infected with the indicated WT alphaviruses (as in Fig. 2a) were evaluated for

the presence of chimeric alphaviruses using both Hela ΔG3BP and U2OS ΔG3BP cells. Vero cells were transduced with SAM vaccine and 1 hour later infected with the WT alphavirus at the indicated MOIs (SAM→WT MOI=1/10 (+1h)). SAM vaccine and WT virus (10 $TCID_{50}$/ml) were added to the Vero cells at the same time (SAM + WT), or Vero cells were infected with the WT alphavirus (10 $TCID_{50}$/ml) and 1 hour later transduced with SAM vaccine (WT→ SAM (+1h)). After 72 hours, supernatants were four times serial passaged on Hela, Hela ΔG3BP, U2OS, and U2OS ΔG3BP cells. No CPE (indicating absence of a chimeric alphavirus) was observed in ΔG3BP cells. **d**, Indicated cell lines were infected with the WT alphaviruses (10 $TCID_{50}$/ml) followed by transduction with SAM vaccine (10 VRPs/cell, 1 hour later). After 72 hours, supernatants were four times passaged on Hela, Hela ΔG3BP, U2OS, and U2OS ΔG3BP cells. No CPE (indicating absence of a chimeric alphavirus) was seen in ΔG3BP cells. **e**, Supernatants from Vero cells infected with the indicated WT alphaviruses followed by transduction with SAM vaccine (10 VRPs/cell, 1 hour later) were four times passaged on U2OS, and U2OS ΔG3BP cells. No CPE (indicating absence of a chimeric alphavirus) was seen in ΔG3BP cells. **f**, Delivery to Vero cells of SAM vaccine (SAM-mCherry) formulated as LNPs (ALC-0315 lipid mix, Echelon Biosciences) or using Lipofectamine-2000 (Thermo). **g,** One step RT-PCR analysis of the SAM-mCherry-GETV chimera (chimera), GETV, and TC-83 using RNA extracted from supernatants. Primers amplify fragments of the TC-83 non-structural protein 2 sequence (nsP2, 150 bp), GETV nsP2 sequence (150 bp), TC-83 structural envelope glycoprotein E2 sequence (100 bp), and GETV E2 sequence (GETV sP, 100 bp). **h**, SDS-PAGE and western blot analysis of SAM-mCherry-GETV chimera (chimera), GETV, and TC-83 infections. Infected cell lysate was heated in SDS sample buffer and loaded onto SDS-PAGE gel. The SDS-PAGE gel was stained by using Coomassie Brilliant Blue (protein stain) and transferred to PVDF membranes followed by western blot detection using goat anti-TC-83 nsP2 (1:1000, AlphaVax), rabbit anti-goat alkaline phosphatase (1:2500, Sigma), alkaline phosphatase, and NBT/BCIP (1:50, Roche).

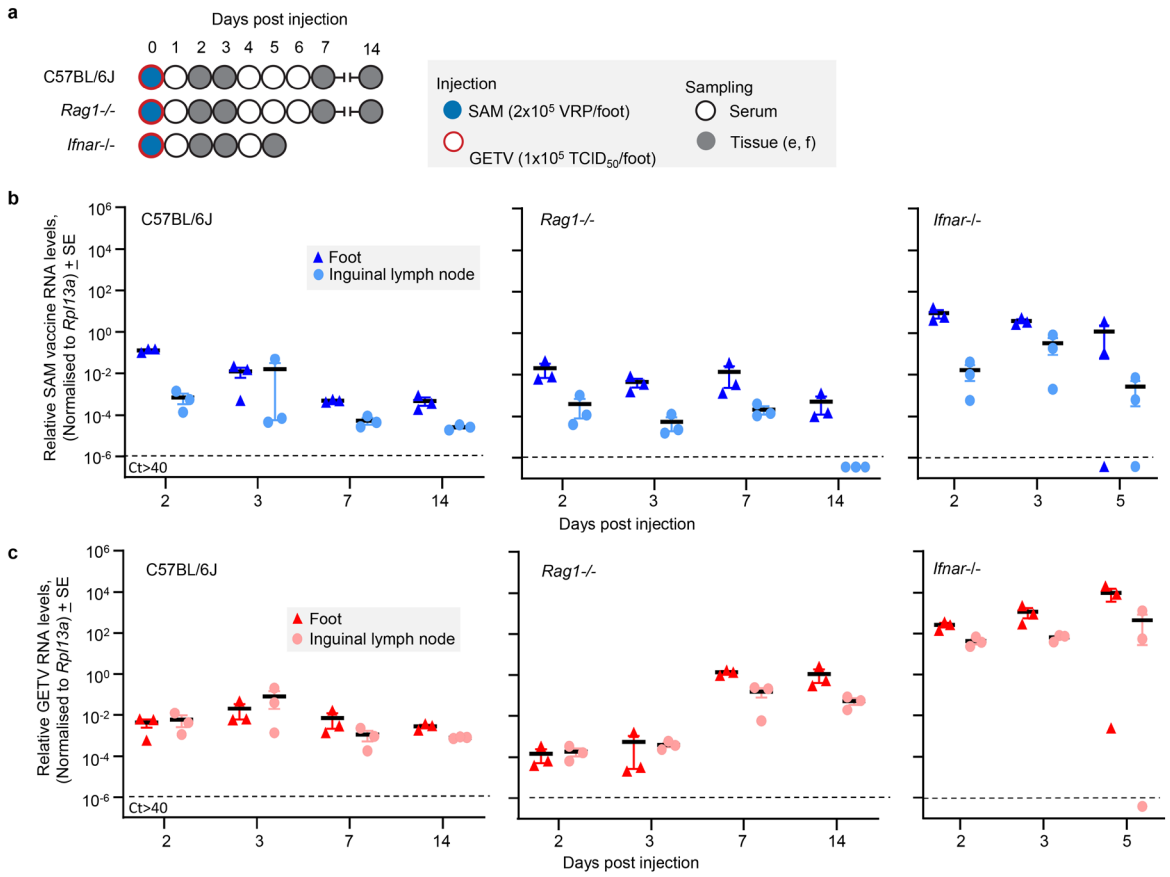

Figure S5. SAM vaccine and GETV co-injection qRT-PCR analyses by tissue and time. **a,** C57BL/6J mice were co-injected subcutaneously into the hind feet with SAM vaccine ($2x10^5$ VRP/foot) and with GETV (10^5 $TCID_{50}$/foot) into hind feet of indicated mouse strains. **b,** SAM vaccine RNA in feet and inguinal lymph nodes detected by qRT-PCR. **c,** GETV RNA in feet and inguinal lymph nodes detected by nsP2 sequence qRT-PCR. C57BL/6J feet on days 2 and 3, *Rag1*$^{-/-}$ feet on days 2, 3 and 14, and *Ifnar*$^{-/-}$ feet on days 2, 3 and 5 were chosen for RNA-Seq as they had the highest consistent levels of RNA for both GETV and SAM vaccine. The persistence of alphavirus RNA in feet of C57BL/6J mice has been reported previously[3,4].

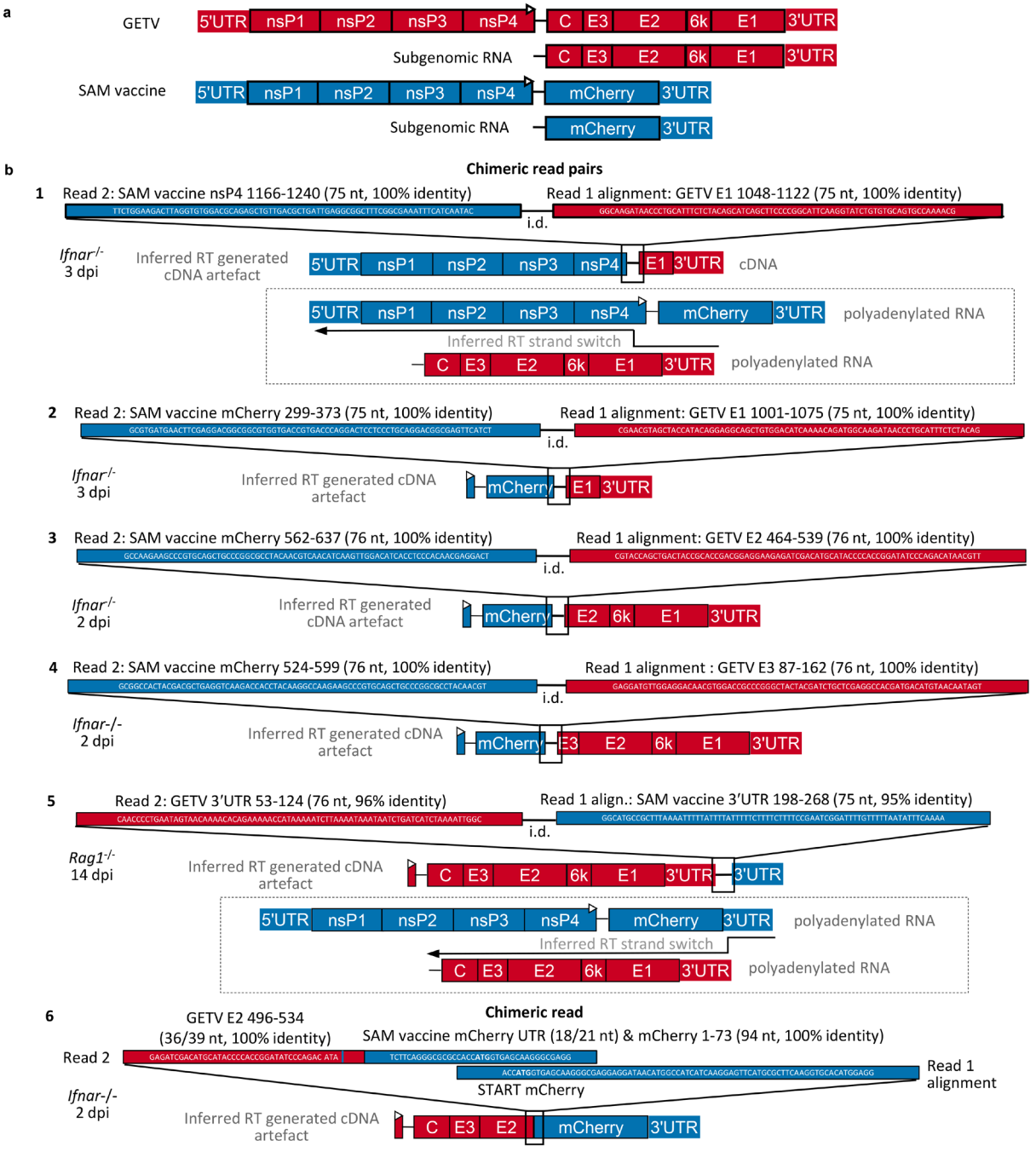

Figure S6. Characterization of alphavirus chimeric read pairs and read. a, Polyadenylated positive strand RNA sequences of GETV and SAM vaccine present in RNA isolated from feet identified by RNA-seq. **b,** Six chimeric read-pairs/read identified from all mouse foot RNA-Seq data (3 mice per group, 3 mouse strains, all times post injection, see Fig. 3a, c). i.d. – inter-read distance. Chimeric cDNA species likely arise as artefacts due to random template switching during reverse-transcription[1] (see Fig. S8). The artefactual chimeric cDNA species and the strand switching events (dashed boxes) can be inferred. To detect chimeric read pairs, alignments (BAMs) were viewed using Samtools to identify paired alignments in which each read in the pair aligned to a different sequence. To detect chimeric reads, read files (Fastqs)

were searched to identify reads containing 22-mers relating to both the GETV and SAM vaccine reference sequences, using an original Python script in Python version 3.7 (original script https://github.com/CameronBishop/detect_chimeric_sequences). Putative chimeric read pairs and reads were subsequently interrogated using Integrative Genomics Viewer version 2.9.4, BioEdit version 7.2.5, Genome Analysis Toolkit version 4.2.4.1 and R version 4.1.0.

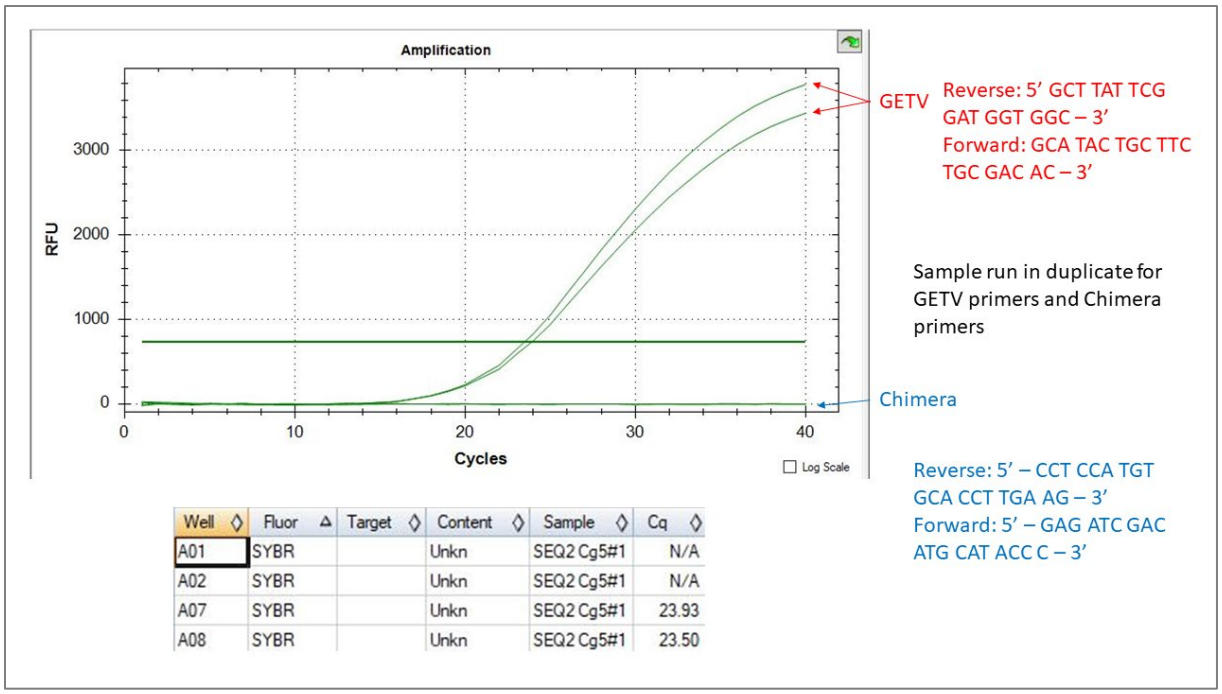

Figure S7. Quantitative RT-PCR detection of putative chimeric reads. Results are shown for the sample (IFNAR mouse 2 dpi) from which chimeric read 6 was obtained. This is the chimeric read with no inter read distance (for details see Fig. S6). Primers were designed to amplify this exact chimeric read. GETV primers served as positive control for qRT-PCR amplification of viral RNA. Chimeric read 6 cannot be amplified and most likely is an artefact.

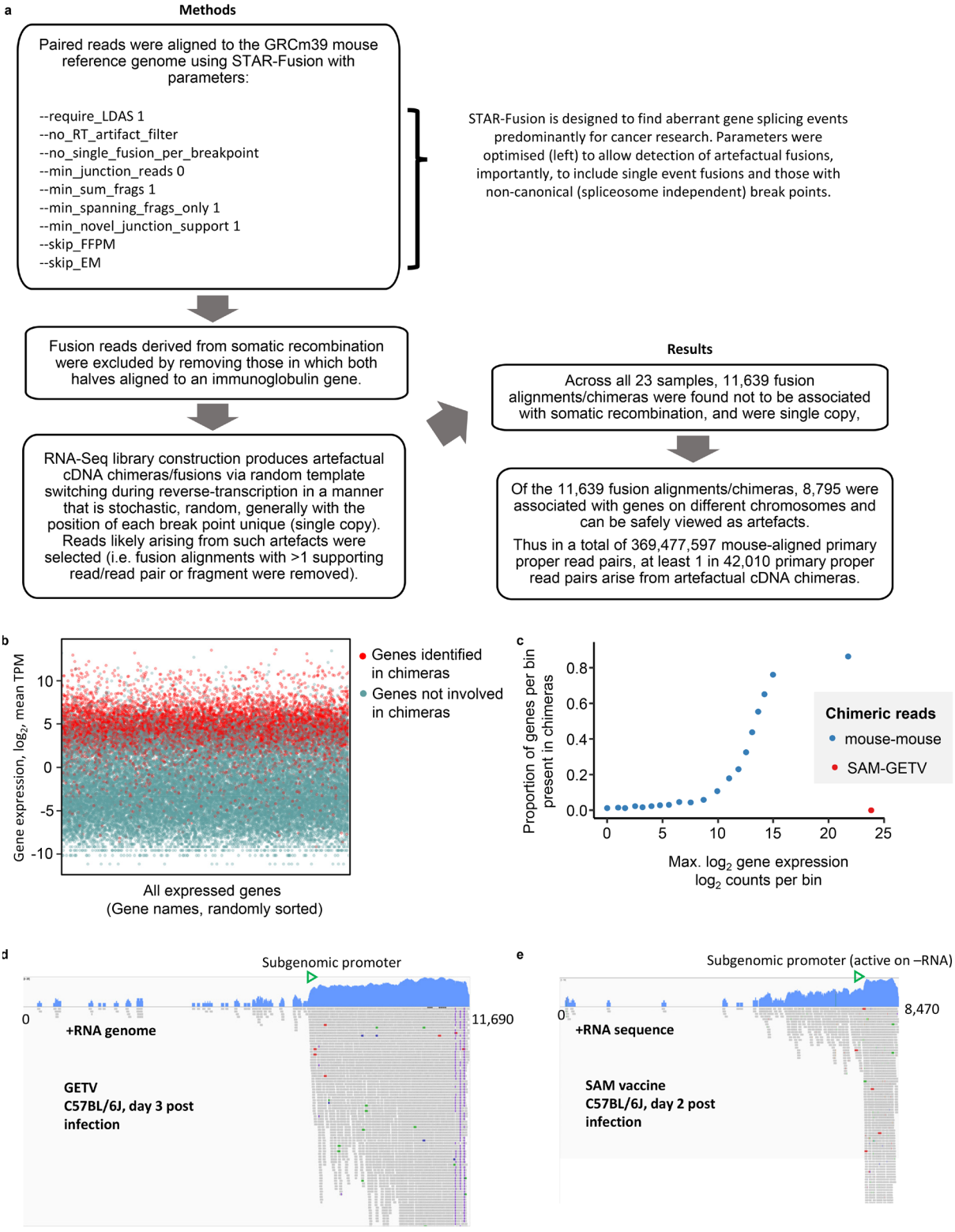

Figure S8. Artefactual mouse chimeric reads generated during cDNA synthesis. a, Process description of STAR-Fusion, illustrating that at least 1 in 42,010 of total mouse reads represent fusion/chimeric read pairs. These likely arise from generation of cDNA artefacts during reverse transcription (RT) [1]. **b**, The expression levels of mouse genes that are present in chimeric reads are higher than expression levels of mouse genes not present in in chimeric reads. **c**, Derived

from b by dividing y axes into 20 bins (and using raw counts rather than TPM). The greater the abundance of an mRNA species (high expression), the greater the chance that it will be incorporated into an artefactual cDNA chimera/fusion during RT. Curve is consistent with a stochastic process[1]. Importantly, the SAM-GETV chimeric read frequency is much lower than the artefactual mouse-mouse chimeric read frequencies. The SAM-GETV chimeric reads are thus highly likely to also be artefacts. **d,** Views of GETV reads aligned to the GETV genome from one mouse. Each grey cigar represents a read. The blue graphs show log read coverage at each nucleotide position (genome is 11, 690 bp). As expected, there are many more reads aligning to the subgenomic RNA encoding the structural genes. The subgenomic promoter operates during synthesis of +RNA from a -RNA template. The less abundant full length +RNA (also generated from the –RNA template) is initiated at the 3′UTR. **e**, As for (d) but for SAM vaccine alignments, where the subgenomic promoter drives production of +RNA carrying the GOI (mCherry).

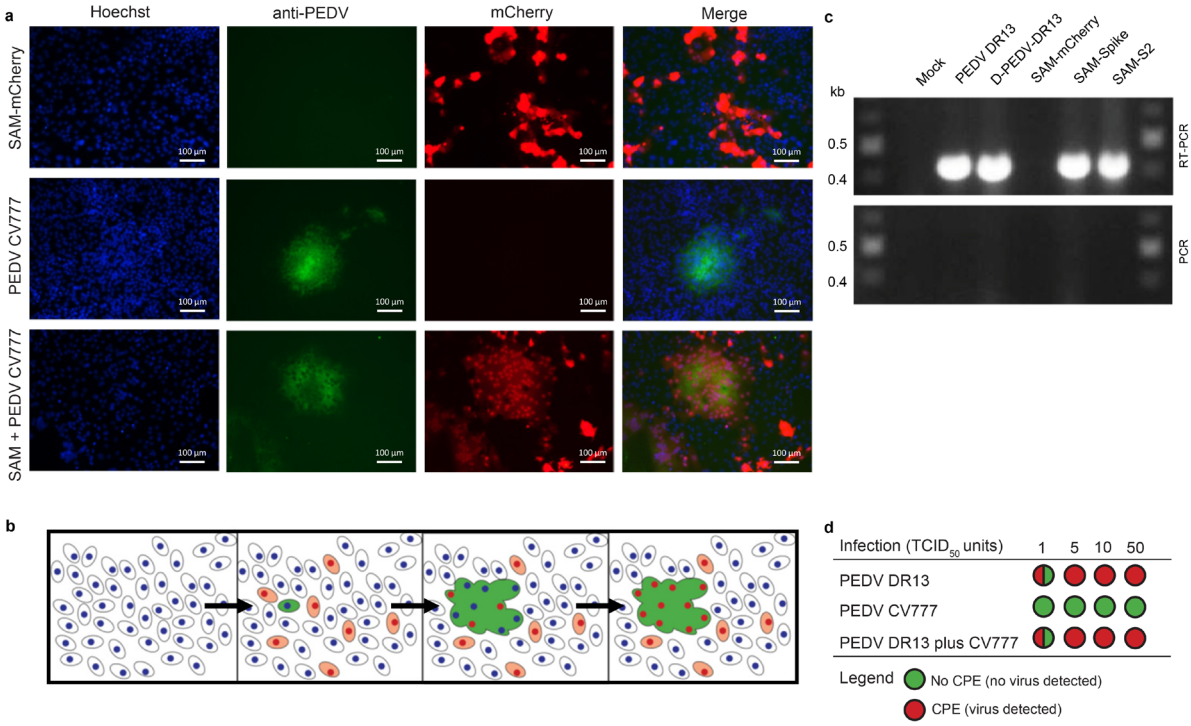

Figure S9. Evaluating recombination between PEDV CV777 and SAM vaccine. a, Fluorescence microscopy of co-transfected/infected Vero cell. Vero cells were transfected with SAM vaccine encoding mCherry and infected with PEDV CV777 (0.1 $TCID_{50}$/cell) 24 hours post transfection. Cell nuclei were stained with Hoechst, PEDV CV777 stained with mouse anti-PEDV spike, and SAM vaccine was visualized by expression of mCherry. **b**, Schematic representation of the development of PEDV CV777 syncytia expressing SAM encoded mCherry. PEDV CV777 infected cells formed large syncytia with SAM-transduced cells. Thereby, the SAM-induced mCherry expression can be detected in the syncytia, visualized by mCherry-positive nuclei in the syncytia. **c**, Detection of spike S2 domain RNA after transfection of SAM templates (SAM-mCherry, SAM-Spike and SAM-S2) and defective PEDV DR13 (D-PEDV-DR13) RNA template in Vero cells. RNA was extracted from cells, DNase treated, and used as input for RT-PCR and PCR analysis using specific spike S2 sequence primers (430 bp product). The presence of the spike RNA after transfection was confirmed by a RT-PCR (amplification of RNA and DNA) product in combination with the absence of a PCR (amplification DNA) product. **d**, Sensitivity of the cell-based coronavirus recombination detection assay. PEDV CV777 was unable to replicate and induce CPE in 10^5 Vero cells in the absence of trypsin, whereas PEDV DR13 was able to replicate and induce CPE within 4 serial passages even at low MOI and in the presence of an excess of PEDV CV777 (10^5 $TCID_{50}$/ml), illustrating the assay's sensitivity and suitability.

References

1 Yan, B. *et al.* Host-virus chimeric events in SARS-CoV-2-infected cells are infrequent and artifactual. *J Virol* **95**, e0029421 (2021). https://doi.org:10.1128/JVI.00294-21

2 Visser, L. J. *et al.* Essential role of enterovirus 2A protease in counteracting stress granule formation and the induction of type I interferon. *J Virol* **93** (2019). https://doi.org:10.1128/JVI.00222-19

3 Poo, Y. S. *et al.* Multiple immune factors are involved in controlling acute and chronic chikungunya virus infection. *PLoS Negl Trop Dis* **8**, e3354 (2014). https://doi.org:10.1371/journal.pntd.0003354

4 Wilson, J. A. *et al.* RNA-Seq analysis of chikungunya virus infection and identification of granzyme A as a major promoter of arthritic inflammation. *PLoS Pathog* **13**, e1006155 (2017). https://doi.org:10.1371/journal.ppat.1006155